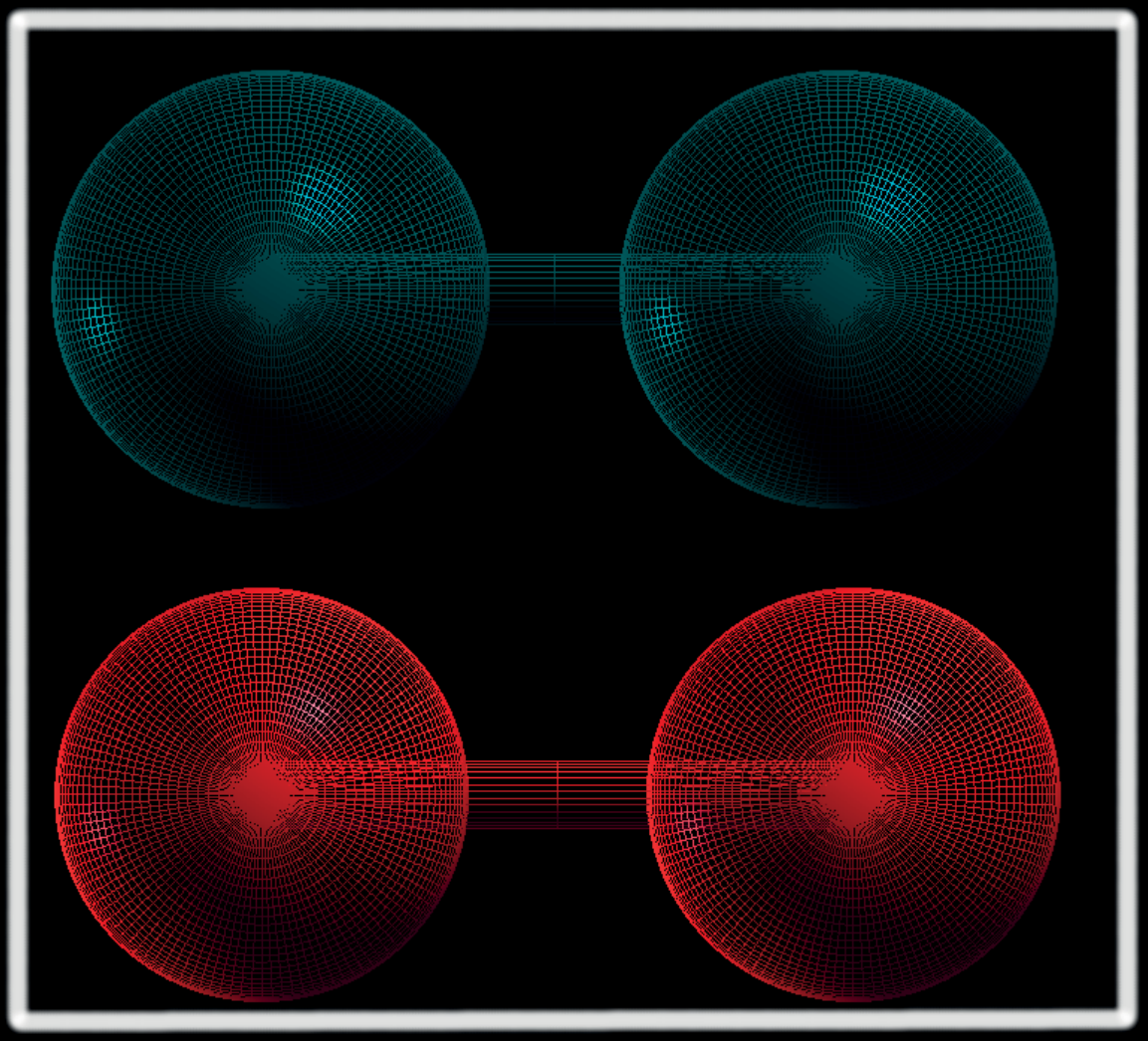

Tiago João Ferreira Gonçalves

OPTICAL AND MAGNETIC PROPERTIES OF TRANSITION METAL CLUSTERS

A thesis submitted in fulfilment of the requirements for the degree of Master of Science in the Centro de Física Computacional, Departamento de Física

September 2015

· U C ·

Universidade de Coimbra

· U C · FCTUC FACULDADE DE CIÊNCIAS E TECNOLOGIA UNIVERSIDADE DE COIMBRA

Master Thesis in Physics

Optical and Magnetic properties of Transition Metal clusters

Author:
Tiago João Ferreira Gonçalves

Supervisors:
Fernando Manuel da Silva Nogueira
Micael José Tourdot de Oliveira

A thesis submitted in fulfilment of the requirements for the degree of Master of Science

in the

Centro de Física Computacional
Departamento de Física

September 2015

"Our virtues and our failings are inseparable, like force and matter. When they separate, man is no more."

Nikola Tesla

Abstract

This Thesis work is based on the study of magnetic and optical properties of transition metal clusters in which some elements of the transition metal section of the periodic table are studied, such as Chromium and Iron. The magnetism of these kind of metals is evaluated on the d-block and these materials will have ferromagnetic or antiferromagnetic properties. The conclusion can be taken by doing the geometry optimization in which we find the geometry and magnetic moment of the cluster on the minimal energy by using *DFT*, after, it is employed the time-dependent *DFT* in order to obtain the optical absorption spectra of the clusters ...

Resumo

O trabalho desta Tese baseia-se no estudo de propriedades ópticas e magnéticas dos aglomerados de metais de transição em que alguns dos elementos desta secção da tabela periódica são estudadas, tais como o Crómio e Ferro. O magnetismo desse tipo de metais é avaliado no bloco d e estes materiais têm propriedades ferromagnético ou antiferromagnético. A conclusão pode ser tomada fazendo a optimização de geometria em que encontramos a geometria e momento magnético do cluster no mínimo de energia usando *DFT*, depois, é usada a *DFT* dependente do tempo de forma a obter os espectros de absorção óptica dos aglomerados ...

Acknowledgements

First of all, I would like to thank my supervisors, professor *Fernando Nogueira* and *Micael Oliveira* that always were available to enlighten and answer to my doubts and questions.

Also, I would like to thank everyone from the *Center of Computational Physics* for the awesome community, specially the mutual aid spirit.

I would like to thank everybody in the department of physics for those five marvelous years.

I Acknowledge all my friends from Coimbra and Ansião for being there whenever I needed to, by providing entertainment on my break times, I would also like to thank them for believing in me.

I Acknowledge my high school professor *Jorge Marques* for all the motivation and "kick start" to the field of physics.

For my girlfriend, thank you for enduring my bad mood on these hard days and I am sorry.

At last but not the least, I would like to thank my family, specially my mother and stepfather for all the support and motivation and my little brother for all the adventures and warm reception every weekend.

Contents

Abstract iii

Acknowledgements v

Contents vii

List of Figures ix

List of Tables xi

Abbreviations xiii

1 Introduction 1

2 N electron Many-Body problem 3
2.1 Non Interacting System . . . 3
2.2 Multiple Electron System . . . 4
2.2.1 Born-Oppenheimer approximation . . . 5
2.3 Many-Body Schrödinger equation . . . 9
2.3.1 Time-dependent Schrödinger equation . . . 9
2.3.2 Density operator . . . 9

3 Density Functional Theory 11
3.1 Importance of DFT . . . 11
3.2 Hohenberg-Kohn Theorems . . . 11
3.3 Kohn-Sham equations . . . 15
3.3.1 The Kohn-Sham approach . . . 15
3.3.2 Relativistic Kohn-Sham equations . . . 17
3.4 Exchange and Correlation Functionals . . . 20
3.4.1 Local Spin Density Approximation . . . 21
3.4.2 Generalized-Gradient Approximation . . . 22
3.4.2.1 Explicit PBE form . . . 23
3.4.3 Non-collinear Spin Density . . . 24

4 Time-Dependent Density Functional Theory 25
4.1 Introduction to TDDFT . . . 25

4.2 The Runge-Gross Theorem . . . 25
4.3 Time-Dependent Kohn-Sham Equations . . . 30
4.3.1 Adiabatic approximation . . . 31
4.4 Linear Response Theory . . . 31
4.4.1 Dynamic polarizability tensor . . . 32
4.4.1.1 Spin-dependent polarizability tensor . . . 35

5 Pseudopotentials **39**
5.1 The Pseudopotential formulation . . . 39
5.2 Norm-conserving pseudopotentials . . . 40
5.2.1 Relativistic effects . . . 42
5.3 The Projector Augmented Wave Method . . . 43

6 Methodology and Results **45**
6.1 Methodology . . . 45
6.2 Results . . . 48
6.2.1 Dimers . . . 49
6.2.1.1 Chromium . . . 49
6.2.1.2 Manganese . . . 53
6.2.1.3 Iron . . . 55
6.2.1.4 Cobalt . . . 59

7 Conclusion **61**

Bibliography **63**

List of Figures

6.1 Example of Cr_2 dimer geometry built on *Avogadro* 45
6.2 Chromium spectra convergence with values of spacing of 0.16, 0.14, 0.12, 0.11, 0.10 and 0.09 $\mathring{A}$. 47
6.3 Chromium spectra convergence with values of radius 5, 6, 7 and 8 $\mathring{A}$. . . . 48
6.4 Absorption Spectrum for Cr_2 with $m_z = 0$ 50
6.5 Absorption Spectra for Cr_2 with $m_z = 0$, using different exchange and correlation functionals, LDA on the green line and GGA on the red one . 51
6.6 Chromium dimer bond length comparison with different magnetizations where the blue dimer represents the Cr_2 with $m_z = 2$ and the red one represents Cr_2 with $m_z = 0$ 52
6.7 Absorption Spectrum for Cr_2 with $m_z = 2$ 52
6.8 Comparison between absorption spectra for Cr_2 with $m_z = 0$ and $m_z = 2$ 53
6.9 Absorption Spectrum for Mn_2 with $m_z = 0$ 54
6.10 Manganese dimer bond length comparison with different magnetizations where the blue dimer represents the Mn_2 with $m_z = 2$ and the red one represents Mn_2 with $m_z = 0$ 55
6.11 Absorption Spectrum for Fe_2 with $m_z = 0$ 56
6.12 Iron dimer bond length comparison with different magnetizations where the blue dimer represents the Fe_2 with $m_z = 2$ and the red one represents Fe_2 with $m_z = 0$ 57
6.13 Absorption Spectrum for Fe_2 with $m_z = 2$ 58
6.14 Comparison between absorption Spectra for Fe_2 with $m_z = 0$ and $m_z = 2$ 58
6.15 Absorption Spectrum for Co_2 with $m_z = 0$ 60

List of Tables

6.1 Chromium properties for a null magnetization 49
6.2 Chromium properties for a given magnetization 51
6.3 Manganese properties for a null magnetization 54
6.4 Manganese properties for a given magnetization 55
6.5 Iron properties for a null magnetization 56
6.6 Iron properties for a given magnetization 57
6.7 Cobalt properties for a null magnetization 59

Abbreviations

MB	**M**any **B**ody
WF	**W**ave**F**unction
TD	**T**ime-**D**ependent
DFT	**D**ensity **F**unctional **T**heory
TDDFT	**T**ime-**d**ependent **D**ensity **F**unctional **T**heory
HK	**H**ohenberg-**K**ohn
KS	**K**ohn-**S**ham
RKS	**R**elativistic **K**ohn-**S**ham
XC	e**X**change and **C**orrelation
LDA	**L**ocal **D**ensity **A**pproximation
LSDA	**L**ocal **S**pin **D**ensity **A**pproximation
GGA	**G**eneralized **G**radient **A**pproximation
ALDA	**A**diabatic **L**ocal **D**ensity **A**pproximation
AGGA	**A**diabatic **G**eneralized **G**radient **A**pproximation
RG	**R**unge-**G**ross
PP	**P**seudo**P**otential
NCPP	**N**orm-**C**onserving **P**seudo**P**otential
PAW	**P**rojector **A**ugmented **W**ave
APE	**A**tomic **P**seudopotentials **E**ngine

Dedicated to my Family and Friends...

Chapter 1

Introduction

Studying optical and magnetic properties of a given material has great advantages on the industry level, because knowing the total magnetization of a cluster, for instances, will give the information regarding its magnetic properties, such as if the cluster has ferromagnetic or anti-ferromagnetic behaviour. So, if we know the informations of the ground-state of the cluster, then we calculate the absorption spectra of that material and since we can achieve different total magnetic moments within the same cluster, then it is expected to have different absorption spectra, i.e. it is spin-dependent, so we face a whole new level of electronics, adding the spin degree of freedom, also called *Spintronics*. Let us imagine that we could read information by simply focus electromagnetic radiation on a material in order to know its magnetization and, consequently, know if we have zero or one, in which both of them corresponds to the binary digit.

Other applications of *Spintronics* are the reading of data in hard disk drives, biosensors, microelectromechanical systems by using the *Giant Magnetoresistive Effect*, in which consists on an effect observed in artificial thin-film materials composed of alternate ferromagnetic and nonmagnetic layers, where the resistance is lowest when the magnetic moments in ferromagnetic layers are aligned and highest when they are antialigned. As the magnetization in the two layers change from parallel to antiparallel alignment, the resistance rises typically from 5 to 10 % . Giant Magnetoresistive multilayer structures are also used in magnetoresistive random-acess memory (MRAM) as cells that store one bit of information.

In this work, *Density Functional Theory* will be used in order to do *ab initio* calculations to extract the ground state properties of the cluster and also optimize the geometry. After, *Time-dependent Density Functional Theory* will be used along with the geometry that was obtained in order to extract information regarding the excited states of the clusters with an electric perturbation and consequently obtain the *Absorption Optical Spectra*.

Chapter 2

N electron Many-Body problem

The Many-Body problem is the background of the fundamental theories that study the electronic structure of atoms, clusters and large scale materials. This chapter will then introduce fundamental definitions and expressions, including the most basic forms valid for Many-body systems of interacting electrons, also simplified formulas valid for non-interacting particles.

2.1 Non Interacting System

In order to understand the Many-Body problem, it is essential to take a look at the simplest case first, in which we consider the Hamiltonian of non interacting particles defined by

$$\hat{H}(x_1, x_2, ..., x_N, t) = \sum_{i=1}^{N} \frac{p_i^2}{2m_i} + \hat{V}(x_1, x_2, x_N, t) \ . \tag{2.1}$$

As we can observe, the first term on the right-hand side represents the total kinetic energy of the system and the potential V specifies the interaction of the particles with any external forces, once again, assuming that the particles do not interact with each other, each particle moves in a common potential so

$$\hat{V}(x_1, x_2, ..., x_N, t) = \sum_{i=1}^{N} \hat{v}(x_i, t) \ . \tag{2.2}$$

Consequently we have

$$\hat{H}(x_1, x_2, ..., x_N, t) = \sum_{i=1}^{N} H_i(x_i, t) \ , \tag{2.3}$$

with $H_i = \frac{p_i^2}{2m_i} + v(x_i, t)$. Knowing that $p_i = i\hbar\frac{d}{dx_i}$, the Hamiltonian of a particle can be rewritten as

$$H_i = -\frac{\hbar^2\nabla_i^2}{2m_e} + \hat{v}(x_i, t) \ . \tag{2.4}$$

So if we consider a system with non-interacting particles, it is safe to say that this system behaves like a set of N 1-particle independent systems.

2.2 Multiple Electron System

If we consider a system with many electrons, it is unrealistic to assume that an electron does not interact with another one and/or with the nuclei. So for the simplest Many Body problem, relativistic effects, magnetic fields and quantum electrodynamics are not included, so the Hamiltonian can be written as

$$\hat{H} = \hat{T} + \hat{V}_{ext} + \hat{V}_{int} + \hat{T}_{core} + E_{II} \ . \tag{2.5}$$

Adopting Hartree atomic units, $\hbar = e = m_e = \frac{4\pi}{\epsilon_0} = 1$, the terms can be written in a simpler form. For the kinetic energy operator for the electrons $\hat{T}$ we have

$$\hat{T} = \sum_i -\frac{1}{2}\nabla_i^2 \ . \tag{2.6}$$

The potential acting on the electrons due to the nuclei is defined by

$$\hat{V}_{ext} = \sum_{i,I} V_I(|\mathbf{r}_i - \mathbf{R}_I|) \ . \tag{2.7}$$

The electron-electron Coulomb interaction is then given by

$$\hat{V}_{int} = \frac{1}{2}\sum_{i\neq j} \frac{1}{|\mathbf{r}_i - \mathbf{r}_j|} \ , \tag{2.8}$$

where the factor $1/2$ exists in order to avoid double counting.
At last, the kinetic energy operator of the nuclei can be written as

$$\hat{T}_{core} = -\sum_{I} \frac{1}{2M_I} \nabla_I^2 \ . \tag{2.9}$$

The final term E_{II} is the interaction of nuclei with one another and any other terms that contribute to the total energy of the system but not pertinent to the problem of describing the electrons. In this term, it is also included the effect of nuclei on electrons in a fixed potential *external* to them, after considering the Born-Oppenheimer approximation described in the subsection 2.2.1. It is also important to take into account that this general form also applies if the bare Coulomb interaction is replaced by a pseudopotential that includes effects of core electrons. So the Hamiltonian of a multiple electron system is given by

$$\hat{H} = -\frac{1}{2}\sum_{i} \nabla_i^2 - \sum_{i,I} \frac{Z_1}{|\mathbf{r}_i - \mathbf{R}_I|} + \frac{1}{2}\sum_{i \neq j} \frac{1}{|\mathbf{r}_i - \mathbf{r}_j|} - \sum_{I} \frac{1}{2M_I} \nabla_I^2 + \frac{1}{2}\sum_{I \neq J} \frac{Z_I Z_J}{|\mathbf{R}_I - \mathbf{R}_J|} \ , \tag{2.10}$$

in which, the electrons are denoted as lower case subscripts and nuclei, with charge Z_I and mass M_I, are denoted as upper case subscripts.

2.2.1 Born-Oppenheimer approximation

It is hard to come up with an exact solution of the Hamiltonian obtained from equation (2.10), so an approximation is required in order to simplify the problem. Taking into account the mass of an electron is much lower than a proton's, with a ratio of the order of 1800 times, then it is safe to consider the motion of the electrons for a frozen nuclei. So the term in the Hamiltonian that corresponds to the equation (2.9) is the smallest term and will be treated as a perturbation.

Taking into account that $\mathbf{r}$ and $\mathbf{R}$ are a set of all-electron and all nuclear coordinates respectively then the full solutions for the coupled system of nuclei and electrons are given by

$$\hat{H}\ \Psi_s(\mathbf{r}, \mathbf{R}) = E_s\ \Psi_s(\mathbf{r}, \mathbf{R}) \ , \tag{2.11}$$

being s the states of the coupled system. Since we assume that the nuclei is frozen, then $\mathbf{R}$ is just a parameter in $\psi_k(\mathbf{r}, \mathbf{R})$. The wavefunctions for a given state of the coupled

electron-nuclear system can be splitted into a function of the nuclear coordinates and the electronic wavefunction as it can be seen in equation (2.12), also $E_k(\mathbf{R})$ and $\psi_k(\mathbf{r},\mathbf{R})$ are the *eigenvalues* and *wavefunctions* for the electrons.

$$\Psi_s(\mathbf{r},\mathbf{R}) = \sum_k \chi_{sk}(\mathbf{R})\ \psi_k(\mathbf{r},\mathbf{R})\ . \tag{2.12}$$

Inserting now the expansion (2.12) into (2.11) knowing that $\hat{H}$ is given by the equation (2.10) we get

$$\hat{H}\Psi(\mathbf{r},\mathbf{R}) = \alpha+\beta+\gamma+\Delta+\Omega = E_s\sum_k \chi_{sk}(\mathbf{R})\ \psi_k(\mathbf{r},\mathbf{R})\ . \tag{2.13}$$

With α, β, γ, Δ and Ω defined by

$$\alpha = -\frac{1}{2}\sum_k\sum_i \nabla_i^2[\ \chi_{sk}(\mathbf{R})\ \psi_k(\mathbf{r},\mathbf{R})\ ]\ , \tag{2.14}$$

$$\beta = -\frac{1}{2}\sum_j\sum_I \frac{1}{M_I}\nabla_I^2[\ \chi_{sk}(\mathbf{R})\ \psi_k(\mathbf{r},\mathbf{R})\ ]\ , \tag{2.15}$$

$$\gamma = -\sum_k\sum_i\sum_I \frac{Z_I}{|\mathbf{r}_i-\mathbf{R}_I|}\ \psi_k(\mathbf{r},\mathbf{R})\ \chi_{sk}(\mathbf{R})\ , \tag{2.16}$$

$$\Delta = \sum_k\sum_{i\neq j} \frac{1}{|\mathbf{r}_i-\mathbf{r}_j|}\ \psi_k(\mathbf{r},\mathbf{R})\ \chi_{sk}(\mathbf{R})\ , \tag{2.17}$$

$$\Omega = \sum_k\sum_{I\neq J} \frac{Z_I Z_J}{|\mathbf{R}_I-\mathbf{R}_J|}\ \psi_k(\mathbf{r},\mathbf{R})\ \chi_{sk}(\mathbf{R})\ . \tag{2.18}$$

Since the term α has no sum over the nuclei, therefore we can isolate $\chi_{sk}(\mathbf{R})$ turning equation (2.14) into

$$\alpha = -\frac{1}{2}\sum_k \chi_{sk}(\mathbf{R})\sum_i \nabla_i^2\ \psi_k(\mathbf{r},\mathbf{R})\ . \tag{2.19}$$

Adding now α with γ, Δ and integrating, we get

$$\alpha + \gamma + \Delta = \sum_k \chi_{sk}(\mathbf{R}) \int \mathrm{d}\mathbf{r}\ \psi_k^*(\mathbf{r},\mathbf{R})\ E_k\ \psi_k(\mathbf{r},\mathbf{R})\ . \tag{2.20}$$

Being

$$E_k|\psi_k\rangle = \left[-\frac{1}{2}\sum_i \nabla_i^2 - \sum_i \sum_I \frac{Z_I}{|r_i - R_I|} + \sum_{i\neq j} \frac{1}{|r_i - r_j|}\right] |\psi_k\rangle\ . \tag{2.21}$$

In order to integrate β, we have to pay special attention, because there is a sum over the nuclei $\sum_I$ and consequently the term $\chi_{sk}(\mathbf{R})$ cannot be isolated. So

$$\beta = -\frac{1}{2}\sum_k \sum_I \frac{1}{M_I} \int \mathrm{d}\mathbf{r}\ \psi_k^*(\mathbf{r},\mathbf{R})\ \rho\ , \tag{2.22}$$

with ρ being

$$\begin{aligned} \rho\ &= \nabla_I^2\ \chi_{sk}(\mathbf{R})\ \psi_k(\mathbf{r},\mathbf{R}) + \chi_{sk}(\mathbf{R})[\ \nabla_I^2\ \psi_k(\mathbf{r},\mathbf{R})] + \\ &+ 2[\ \nabla_I\ \chi_{sk}(\mathbf{R})\ ][\ \nabla_I\ \psi_k(\mathbf{r},\mathbf{R})\ ]\ . \end{aligned} \tag{2.23}$$

Finally, (2.11) can be rewritten as

$$\left[\sum_I -\frac{\nabla_I^2}{2M_I} + E_k(\mathbf{R}) - E_s\right] \chi_{si}(\mathbf{R}) = -\sum_{k'} \left[A_{kk'}(\mathbf{R}) + B_{kk'}(\mathbf{R})\right] \chi_{si'}(\mathbf{R})\ , \tag{2.24}$$

where the matrix elements $A_{kk'}(\mathbf{R})$ and $B_{kk'}(\mathbf{R})$ are given by

$$A_{kk'}(\mathbf{R}) = -\sum_I \frac{1}{M_I} \int \mathrm{d}\mathbf{r}\ \left[\psi_k^*(\mathbf{r},\mathbf{R})\ \vec{\nabla}_I\ \psi_{k'}(\mathbf{r},\mathbf{R})\right].\vec{\nabla}_I\ , \tag{2.25}$$

$$B_{kk'}(\mathbf{R}) = -\frac{1}{2}\sum_I \frac{1}{M_I} \int \mathrm{d}\mathbf{r}\ \psi_k^*(\mathbf{r},\mathbf{R})\ \nabla_I^2\ \psi_{k'}(\mathbf{r},\mathbf{R})\ . \tag{2.26}$$

So, the *Born-Oppenheimer approximation* consists on ignoring the off-diagonal terms of the matrix elements $A_{kk'}(\mathbf{R})$ and $B_{kk'}(\mathbf{R})$ as these can be much smaller compared to the nuclei kinetic energy. This means that as the nuclei move, electrons tend to remain in a given state knowing, however, that the electron wavefunction and the energy of a

given state changes and so, we may conclude that no energy is transferred between the degrees of freedom described by the equation for the nuclear variables $\mathbf{R}$ and excitations of the electrons, which only occurs if there is a change of state [3] [29].

2.3 Many-Body Schrödinger equation

2.3.1 Time-dependent Schrödinger equation

It is important to mention and understand the time-dependent Schrödinger equation for the *Many-Body* problem because after the introduction to *Density Functional Theory*, this is the basis of time-dependent DFT in which molecular excitation spectra and optical response will be studied.

So, on a non-relativistic quantum system, the time-dependent Schrödinger equation can be written as

$$\mathrm{i}\frac{d\Psi(\mathbf{r}_i;t)}{dt} = \hat{H}(\mathbf{r}_i;t)\ \Psi(\mathbf{r}_i;t)\ , \tag{2.27}$$

where $\Psi(\mathbf{r}_i;t)$ represents the *Many-Body* wavefunction for the electrons, once again, $\mathbf{r}_i$ represents a set of coordinates of the electrons $\mathbf{r}_1, \mathbf{r}_2, ..., \mathbf{r}_N$ in which the spin is included also, since electrons are fermions, then the wavefunction must be antisymmetric in those coordinates, which means

$$\Psi(\mathbf{r}_1, \mathbf{r}_2, ..., \mathbf{r}_N; t) = -\Psi(\mathbf{r}_N, ..., \mathbf{r}_2, \mathbf{r}_1; t)\ . \tag{2.28}$$

2.3.2 Density operator

Since the density of particles $n(\mathbf{r})$ plays an important role on DFT, it is worth mentioning that it is given by the expectation value of the density operator

$$\hat{n}(\mathbf{r}) = \sum_{i=1}^{N} \delta(\mathbf{r} - \mathbf{r}_i)\ , \tag{2.29}$$

$$n(\mathbf{r}) = \sum_{i=1}^{N} \int \mathrm{d}\mathbf{r}_1\ \mathrm{d}\mathbf{r}_2\ ...\ \mathrm{d}\mathbf{r}_\mathrm{N}\ \delta(\mathbf{r} - \mathbf{r}_i)|\Psi(\mathbf{r}_1, \mathbf{r}_2, ..., \mathbf{r}_N)|^2\ , \tag{2.30}$$

being $\delta(\mathbf{r} - \mathbf{r}_i)$ the *Kronecker delta*. We can also write equation (2.30) in this way

$$\begin{aligned} n(\mathbf{r}) = &\int \mathrm{d}\mathbf{r}_2\ \mathrm{d}\mathbf{r}_3\ ...\ \mathrm{d}\mathbf{r}_\mathrm{N}\ |\Psi(\mathbf{r}, \mathbf{r}_2, \mathbf{r}_3, ..., \mathbf{r}_N)|^2 + \\ &+ \int \mathrm{d}\mathbf{r}_1\ \mathrm{d}\mathbf{r}_3\ ...\ \mathrm{d}\mathbf{r}_\mathrm{N}\ |\Psi(\mathbf{r}_1, \mathbf{r}, \mathbf{r}_3, ..., \mathbf{r}_N)|^2 + ...\ . \end{aligned} \tag{2.31}$$

In order to simplify (2.31), we can integrate the equation with the Kronecker delta acting always on the same coordinate $\mathbf{r}_1$ and we get as a result

$$n(\mathbf{r}) = N \int \mathrm{d}\mathbf{r}_2 \; \mathrm{d}\mathbf{r}_3 \; ... \; \mathrm{d}\mathbf{r}_\mathrm{N} \; |\Psi(\mathbf{r}, \mathbf{r}_2, \mathbf{r}_3, ..., \mathbf{r}_N)|^2 \; . \tag{2.32}$$

At last, in order to normalize the density of particles

$$n(\mathbf{r}) = N \frac{\int \mathrm{d}\mathbf{r}_2 \; \mathrm{d}\mathbf{r}_3 \; ... \; \mathrm{d}\mathbf{r}_\mathrm{N} \; \sum_{\sigma_1} |\Psi(\mathbf{r}, \mathbf{r}_2, \mathbf{r}_3, ..., \mathbf{r}_N)|^2}{\int \mathrm{d}\mathbf{r}_1 \; \mathrm{d}\mathbf{r}_2 \; \mathrm{d}\mathbf{r}_3 \; ... \; \mathrm{d}\mathbf{r}_\mathrm{N} \; |\Psi(\mathbf{r}_1, \mathbf{r}_2, \mathbf{r}_3, ..., \mathbf{r}_N)|^2} \; . \tag{2.33}$$

Where $\sum_{\sigma_1}$ represents a sum over the z-component of spin. For a closer look of this chapter, see [1], [2], [3] and [31].

Chapter 3

Density Functional Theory

3.1 Importance of DFT

One of the basic problems in theoretical physics and chemistry is the description of the structure and dynamics of many electron systems. Many approaches are considered in order to solve these kind of systems however, density functional theory is a completely different, formally rigorous, way of approaching any interacting problem by mapping it exactly to a much easier to solve non-interacting problem. Its methodology is applied in a large variety of fields to many different problems, with the ground state electronic structure problem simply being the most common. Also the remarkable successes of local density approximation (LDA) and generalized-gradient approximation (GGA) functionals [17] within the Kohn-Sham approach have led to a widespread interest in DFT as the most promising approach for accurate, practical methods in the theory of materials.

3.2 Hohenberg-Kohn Theorems

By solving the Scrödinger equation for the eigenstates of the system, it is evident the external potential in principle determines all properties of the system, so the main objective of Hohenberg and Kohn is to formulate density functional theory as an exact theory of Many-Body systems. So taking a look into the Hamiltonian of the system

$$\hat{H} = \hat{T} + \hat{V}_{\text{ext}} + \hat{V}_{\text{ee}} \ , \tag{3.1}$$

in which $\hat{T}$, $\hat{V}_{\text{ext}}$ and $\hat{V}_{\text{ee}}$ represents the kinetic energy, the external potential and the electron-electron interaction respectively:

$$\hat{T} = -\frac{1}{2}\sum_i \nabla_i^2 \ , \tag{3.2}$$

$$\hat{V}_{\text{ext}} = \sum_i v_{\text{ext}}(\mathbf{r}_i) = \int \mathrm{d}\mathbf{r}\ v_{\text{ext}}(\mathbf{r})\ \hat{n}(\mathbf{r}) \ , \tag{3.3}$$

$$\hat{V}_{\text{ee}} = \sum_{i\neq j} \frac{1}{|\mathbf{r}_i - \mathbf{r}_j|} \ . \tag{3.4}$$

It is important to note that the set of all local potentials on the Hamiltonian (3.1) will lead to a non-degenerate ground state eigenfunction.

The first theorem states that the particle density of the ground state $n(\mathbf{r}_0)$, determines uniquely the external potential $\hat{V}_{\text{ext}}$, except for a constant. Now in order to prove this first theorem, we need to reduce to absurdity. Assuming that $|\Psi_0>$ is simultaneously the ground state for two different potentials $v_{\text{ext}}^{(1)}$ and $v_{\text{ext}}^{(2)} \neq v_{\text{ext}}^{(1)} + \text{constant}$, then we may write two Schrödinger equations

$$[\hat{T} + \hat{V}_{\text{ext}}^{(1)} + \hat{V}_{\text{ee}}]\big|\Psi_0\big\rangle = E_0^{(1)}\big|\Psi_0\big\rangle \ , \tag{3.5}$$

$$[\hat{T} + \hat{V}_{\text{ext}}^{(2)} + \hat{V}_{\text{ee}}]\big|\Psi_0\big\rangle = E_0^{(2)}\big|\Psi_0\big\rangle \ . \tag{3.6}$$

If we subtract both equations we achieve

$$[\hat{V}_{\text{ext}}^{(1)} - \hat{V}_{\text{ext}}^{(2)}]\big|\Psi_0\big\rangle = [E_0^{(1)} - E_0^{(2)}]\big|\Psi_0\big\rangle \ . \tag{3.7}$$

Because $v_{\text{ext}}^{(1)}$ and $v_{\text{ext}}^{(2)}$ are different by more than a constant and equation (3.7) states that the difference between both potentials is a mere constant, then we have reached a contradiction. Therefore, each potential v_{ext} that differs from a constant corresponds to a ground state $\big|\Psi_0\big\rangle$.

Now, recalling the density of particles $n(\mathbf{r})$ achieved on subsection 2.3.2 and knowing that the ground state density n_0 is defined by

$$n_0(\mathbf{r}) = \big\langle\Psi_0\big|\hat{n}(\mathbf{r})\big|\Psi_0\big\rangle \ , \tag{3.8}$$

then it is clear that in this equation it is not possible for each $|\Psi_0>$ to have more than one correspondent n_0. In other words, the density set is Injective. To show that the set is indeed injective, we must, once again, reduce to absurdity. Considering two different wavefunctions $\Psi^{(1)}$ and $\Psi^{(2)}$, assuming that both have the same particle density $n_0(\mathbf{r})$ and since $\Psi^{(2)}$ is not the ground state of $\hat{H}^{(1)}$ we have

$$E_0^{(1)} = \left\langle \Psi_0^{(1)} \middle| \hat{H}^{(1)} \middle| \Psi_0^{(1)} \right\rangle < \left\langle \Psi_0^{(2)} \middle| \hat{H}^{(1)} \middle| \Psi_0^{(2)} \right\rangle . \tag{3.9}$$

This inequality follows if the ground state is non-degenerate, also

$$\left\langle \Psi^{(2)} \middle| \hat{H}^{(1)} \middle| \Psi^{(2)} \right\rangle = \left\langle \Psi^{(2)} \middle| \hat{H}^{(2)} \middle| \Psi^{(2)} \right\rangle + \left\langle \Psi^{(2)} \middle| \hat{H}^{(1)} - \hat{H}^{(2)} \middle| \Psi^{(2)} \right\rangle . \tag{3.10}$$

Now, from the relation established from equation (3.9), one can rewrite equation (3.10) as

$$E_0^{(1)} < E_0^{(2)} + \left\langle \Psi^{(2)} \middle| \hat{V}_{\text{ext}}^{(1)} - \hat{V}_{\text{ext}}^{(2)} \middle| \Psi^{(2)} \right\rangle . \tag{3.11}$$

If we use equation (3.3) and also the assumption that both states lead to the same density n_0, we get

$$E_0^{(1)} < E_0^{(2)} + \int \mathrm{d}\mathbf{r}\ n_0(\mathbf{r}) \left[v_{\text{ext}}^{(1)}(\mathbf{r}) - v_{\text{ext}}^{(2)}(\mathbf{r}) \right] . \tag{3.12}$$

On the other hand, if we switch $E_0^{(2)}$ and $E_0^{(1)}$ on equation (3.11), we may find subscripts (1) and (2) interchanged

$$E_0^{(2)} < E_0^{(1)} + \int \mathrm{d}\mathbf{r}\ n_0(\mathbf{r}) \left[v_{\text{ext}}^{(2)}(\mathbf{r}) - v_{\text{ext}}^{(1)}(\mathbf{r}) \right] . \tag{3.13}$$

At last adding both (3.12) and (3.13) we end up with a contradiction as a result, where

$$E_0^{(1)} + E_0^{(2)} < E_0^{(2)} + E_0^{(1)} . \tag{3.14}$$

So, we may conclude that for each potential we get only one $\left|\Psi_0\right\rangle$ and for each $\left|\Psi_0\right\rangle$ we get a correspondent n_0.

Now, the second theorem states that, according to the last theorem, $\left|\Psi_0\right\rangle$, the density of particles and the external potential are related and so, an universal functional for the

energy $E[n]$ can be defined and the global minimum of this functional represents the exact ground state energy of the system for one particular $\hat{V}_{\text{ext}}(\mathbf{r})$ and the density $n(\mathbf{r})$ that minimizes the functional is the exact ground state density $n_o(\mathbf{r})$.
Considering the functional $\big|\Psi[n]\big\rangle$ in which any ground state observable $O[n]$ is a density functional

$$O[n] = \big\langle \Psi[n] \big| \hat{O} \big| \Psi[n] \big\rangle \ . \tag{3.15}$$

Amongst these functionals, the most important one is the ground state energy

$$E_{\text{HK}}[n] = \big\langle \Psi[n] \big| \hat{H} \big| \Psi[n] \big\rangle = F_{\text{HK}}[n] + \int \mathrm{d}\mathbf{r}\ V_{\text{ext}}(\mathbf{r})\ n(\mathbf{r}) + E_{II} \ , \tag{3.16}$$

where E_{II} represents the interaction energy of the nuclei, as mentioned on section 2.2 and $F_{\text{HK}}[n]$ includes all internal kinetic and potential energies

$$F_{\text{HK}}[n] = T[n] + E_{\text{int}} \ . \tag{3.17}$$

Now if we consider a system with the ground state density $n^{(1)}(\mathbf{r})$ that corresponds to an external potential $V^{(1)}_{\text{ext}}(\mathbf{r})$, the Hohenberg-Kohn functional is

$$E_{\text{HK}}[n^{(1)}] = E^{(1)} = \big\langle \Psi^{(1)} \big| \hat{H}^{(1)} \big| \Psi^{(1)} \big\rangle \ . \tag{3.18}$$

If we consider a different density $n^{(2)}(\mathbf{r})$, the expectation value of the Hamiltonian in the unique ground state will have a different wavefunction, like $\Psi^{(2)}$, and so

$$E^{(1)} = \big\langle \Psi^{(1)} \big| \hat{H}^{(1)} \big| \Psi^{(1)} \big\rangle < \big\langle \Psi^{(2)} \big| \hat{H}^{(1)} \big| \Psi^{(2)} \big\rangle = E^{(2)} \ . \tag{3.19}$$

As a result, comparing densities of particles, the Hohenberg-Kohn functional will give the lowest energy if $n(\mathbf{r}) = n_0(\mathbf{r})$. Consequently, knowing the functional $F_{\text{HK}}[n]$, one can minimize the total energy of the system by varying $n(\mathbf{r})$, finding at last, the exact ground state density and energy. In other words, the functional $E[n]$ alone is sufficient to determine those. It, however, will not give any information regarding excited states.

3.3 Kohn-Sham equations

3.3.1 The Kohn-Sham approach

Going back to the Hamiltonian (2.5) with a non-degenerate ground state, in which the HK theorems state that knowing the ground state density is enough to determine all ground state observables, also the ground state energy functional $E[n]$ allows the determination of the ground state density itself via the variational equation

$$\frac{\delta}{\delta n(\mathbf{r})}\left\{E[n]-\mu\left(\int \mathrm{dr}\ n(\mathbf{r})-N\right)\right\}\Bigg|_{n(\mathbf{r})=n_0(\mathbf{r})}=0\ , \tag{3.20}$$

that gives the *Euler-Lagrange equation*[1] with an external potential $v(\mathbf{r})$

$$\mu=\frac{\delta E[n]}{\delta n(\mathbf{r})}=v(\mathbf{r})+\frac{\delta F_{\mathrm{HK}}[n]}{\delta n(\mathbf{r})}\ , \tag{3.21}$$

in which the *minimum principles* will indicate the possibility to determine the ground state density of a many-particle system.

Then, the Kohn-Sham approach is to replace the interacting many-body system obeying the Hamiltonian considered with a different auxiliary system. So, the KS *ansatz* implies that the ground state density of the original interacting system is equivalent to some chosen non-interacting system of the type mentioned back at section 2.1 with all the many-body terms included into an *exchange-correlation functional of the density*, and this is called *non-interacting-V-representability*.

In order to introduce the KS equations, we must consider first a system of non-interacting electrons with a multiplicative external potential v_{s}

$$\hat{H}_s=\hat{T}+\int \mathrm{d}\mathbf{r}\ \hat{n}(\mathbf{r})\ v_s(\mathbf{r})\ , \tag{3.22}$$

where the term $\int dr\ \hat{n}(\mathbf{r})\ v_s(\mathbf{r})$ is the external potential operator $\hat{V}_s$ and the non-degenerate ground state $\big|\Psi_0\big\rangle$ in the N-particle system is the Slater determinant

$$\hat{H}_s\big|\Psi_0\big\rangle=E_{s,0}\big|\Psi_0\big\rangle\ , \tag{3.23}$$

[1] μ is the chemical potential, it also is the Lagrangian multiplier with the constraint $\int \mathrm{dr}\ n(\mathbf{r})=N$

$$\begin{aligned}\left\langle \mathbf{r}_1\sigma_1, ...\mathbf{r}_N\sigma_N \middle| \Psi_0 \right\rangle &= \Psi_0(\mathbf{r}_1\sigma_1, ...\mathbf{r}_N\sigma_N) = \\ = \frac{1}{\sqrt{N!}} \det &\begin{pmatrix} \psi_1(\mathbf{r}_1\sigma_1) & \cdots & \psi_N(\mathbf{r}_1\sigma_1) \\ \vdots & \ddots & \vdots \\ \psi_1(\mathbf{r}_N\sigma_N) & \cdots & \psi_N(\mathbf{r}_N\sigma_N) \end{pmatrix} ,\end{aligned} \tag{3.24}$$

with ψ_i being the energetic lowest solutions of the single-particle Schrödinger equation

$$\left\{ -\frac{1}{2}\nabla^2 + v_s(\mathbf{r}) \right\} \psi_i(\mathbf{r}\sigma) = \epsilon_i \psi_i(\mathbf{r}\sigma) \ . \tag{3.25}$$

The eigenvalues ϵ_i are supposed to be ordered from lowest to highest and ϵ_F is the Fermi energy that is identified with the eigenvalue ϵ_N of the highest occupied single-particle level

$$\epsilon_1 \leq \epsilon_2 \leq \ldots \leq \epsilon_N = \epsilon_{\mathrm{F}} \leq \epsilon_{N+1} \leq \cdots \ , \tag{3.26}$$

in which the kinetic energy is $T_s[n]$ in a system of $N = N^{\uparrow} + N^{\downarrow}$ independent electrons

$$T_s[n] = -\frac{1}{2} \sum_{\sigma} \sum_{i=1}^{N^{\sigma}} \left\langle \psi_i^{\sigma} \middle| \nabla^2 \middle| \psi_i^{\sigma} \right\rangle = -\frac{1}{2} \sum_{\sigma} \sum_{i=1}^{N^{\sigma}} \int \mathrm{d}\mathbf{r} \ \psi_i^{\sigma *}(\mathbf{r}) \ \nabla^2 \ \psi_i^{\sigma}(\mathbf{r}) \ . \tag{3.27}$$

From the HK theory, T is a functional of the total electron density given by the sum of squares of the orbitals for each spin

$$n(\mathbf{r}) = \sum_{\sigma} n(\mathbf{r}, \sigma) = \sum_{\sigma} \sum_{i=1}^{N^{\sigma}} \psi_i^{\sigma *}(\mathbf{r}) \ \psi_i^{\sigma}(\mathbf{r}) \ . \tag{3.28}$$

Also, we need to define a self-interacting Coulomb energy of the electron density $n(\mathbf{r})$

$$E_{\mathrm{Hartree}}[n] = \frac{1}{2} \int \mathrm{d}\mathbf{r}_1 \ \mathrm{d}\mathbf{r}_2 \frac{n(\mathbf{r}_1) \ n(\mathbf{r}_2)}{|\mathbf{r}_1 - \mathbf{r}_2|} \ . \tag{3.29}$$

Putting together the independent-particle system with the true interacting many-body system, we get the definition

$$E_{\mathrm{xc}}[n] = F_{\mathrm{HK}}[n] - (T_s[n] + E_{\mathrm{Hartree}}[n]) \ . \tag{3.30}$$

E_{xc} is the exchange and correlation energy functional, being just the difference between the kinetic and all internal interaction energies, since $F_{\text{HK}} = \langle \hat{T} \rangle + \langle \hat{V}_{\text{int}} \rangle$ is the HK functional.

Now we rewrite the HK expression for the ground state energy functional (3.16) in the form

$$E_{KS} = T_s[n] + \int \mathrm{d}\mathbf{r}\ V_{\text{ext}}(\mathbf{r})\ n(\mathbf{r}) + E_{\text{Hartree}}[n] + E_{II} + E_{xc}[n]\ , \tag{3.31}$$

The result is the KS approach to the full interacting many body problem, where E_{Hartree} was defined in (3.29) as the self-interacting Coulomb energy, V_{ext} is the external potential due to the nuclei and any other external fields and E_{II} is the interaction between the nuclei as was defined on equation (2.5) from the section 2.2.

At last, considering the equation (3.20), we get the effective Hamiltonian

$$H^{\sigma}_{\text{KS}}(\mathbf{r}) = -\frac{1}{2}\nabla^2 + V^{\sigma}_{\text{KS}}(\mathbf{r})\ , \tag{3.32}$$

with $V^{\sigma}_{\text{KS}}(\mathbf{r})$ being

$$V^{\sigma}_{\text{KS}}(\mathbf{r}) = V_{\text{ext}}(\mathbf{r}) + V_{\text{Hartree}}(\mathbf{r}) + V^{\sigma}_{\text{xc}}(\mathbf{r})\ , \tag{3.33}$$

where $V_{\text{Hartree}}(\mathbf{r})$ is the Hartree potential

$$V_{\text{Hartree}}(\mathbf{r}) = \frac{\delta E_{\text{Hartree}}}{\delta n(\mathbf{r}, \sigma)}\ , \tag{3.34}$$

and $V^{\sigma}_{\text{xc}}(\mathbf{r})$ is the *Exchange and Correlation* potential

$$V^{\sigma}_{\text{xc}}(\mathbf{r}) = \frac{\delta E_{\text{xc}}}{\delta n(\mathbf{r}, \sigma)}\ . \tag{3.35}$$

3.3.2 Relativistic Kohn-Sham equations

In order to introduce the RKS equations, it is essential to state the Hohenberg-Kohn theorem for the relativistic case where, for a Lorentz covariant situation, the ground state energy is a unique functional of the ground state four-current

$$E_0[j^{\mu}] = F[j^{\mu}] + \int \mathrm{dx}\ j^{\mu}(x)\ v^{\text{ext}}_{\mu}(x)\ , \tag{3.36}$$

with F being a universal functional of j^μ. Also, all ground state observables can be expressed as unique functionals of the ground state four-current as

$$O[j^\mu] = \left\langle \Psi_0[j^\mu] \middle| \hat{O} \middle| \Psi_0[j^\mu] \right\rangle + \Delta O_{\mathrm{CT}} - VEV \ . \tag{3.37}$$

Counter terms ΔO_{CT} and the subtraction of vacuum expectation values (VEV) are included in order to do a renormalization of the observable.

In a situation where the external potential is electrostatic

$$\{v^\mu_{\mathrm{ext}}(x)\} = \{v^0_{\mathrm{ext}}(x), 0\} \ , \tag{3.38}$$

all ground state variables, including the spatial components of the four-current, are functionals, known or unknown, of the charge density alone

$$\mathbf{j}([n], x) = \left\langle \Psi_0[n] \middle| \hat{\mathbf{j}}(x) \middle| \Psi_0[n] \right\rangle \ . \tag{3.39}$$

Now, the relativistic Kohn-Sham aproach starts the same way as the non-relativistic one, so we can write the four-current and the non-interacting kinetic energy in terms of auxiliary spinor orbitals. If we calculate the four-current of a fermionic system, we get

$$j^\mu(\mathbf{x}) = j^\mu_{\mathrm{vac}}(\mathbf{x}) + j^\mu_{\mathrm{D}}(\mathbf{x}) \ , \tag{3.40}$$

where $j^\mu_{\mathrm{D}}(\mathbf{x})$ is the current due to the occupied orbitals and is defined in this way

$$j^\mu_D(\mathbf{x}) = \sum_{-m<\epsilon_i\leq\epsilon_{\mathrm{F}}} \psi^*_i(\mathbf{x})\gamma^\mu\psi_i(\mathbf{x}) \ . \tag{3.41}$$

The vacuum polarization current $j^\mu_{\mathrm{vac}}(\mathbf{x})$ is given by the solution of a Dirac equation

$$j^\mu_{\mathrm{vac}}(\mathbf{x}) = \frac{1}{2}\left[\sum_{\epsilon_i\leq -m} \psi^*_i(\mathbf{x})\gamma^\mu\psi_i(\mathbf{x}) - \sum_{-m<\epsilon_i} \psi^*_i(\mathbf{x})\gamma^\mu\psi_i(\mathbf{x})\right] \ . \tag{3.42}$$

The non-interacting kinetic energy, with the rest mass term can be written as

$$T_s[j^\mu] = T_{s,\mathrm{vac}}[j^\mu] + T_{s,\mathrm{D}}[j^\mu] \ . \tag{3.43}$$

Also, the non-relativistic kinetic energy will be replaced by its relativistic equivalent

$$-\frac{\nabla^2}{2\mathrm{m}} \rightarrow -\mathrm{i}\boldsymbol{\gamma}\cdot\boldsymbol{\nabla}\ , \tag{3.44}$$

And, as a consequence, γ^μ can be replaced by [2]

$$\gamma^\mu \rightarrow -\mathrm{i}\boldsymbol{\gamma}\cdot\boldsymbol{\nabla} + \mathrm{m}\ . \tag{3.45}$$

The contributions given by j^μ on equation (3.43) will therefore be exchanged by (3.45). Now, in order to get the full KS scheme, we write the ground state energy as

$$E_0[j^\mu] = T_s[j^\mu] + E_{\mathrm{ext}}[j^\mu] + E_{\mathrm{Hartree}}[j^\mu] + E_{\mathrm{xc}}[j^\mu]\ , \tag{3.46}$$

being $E_{\mathrm{xc}}[j^\mu]$ the exchange and correlation energy defined as the difference between the universal functional of j^μ and the sum of the non-interacting kinetic energy with the Hartree energy

$$E_{\mathrm{xc}} = F - T_s - E_{\mathrm{Hartree}}\ . \tag{3.47}$$

As was mentioned on non-relativistic KS equations, all the many-body interaction effects are included in the *Exchange and Correlation* energy.
Minimization of the ground state energy with respect to the auxiliary spinor orbitals will lead to a Dirac equation

$$\gamma^0\{-\mathrm{i}\boldsymbol{\gamma}\cdot\boldsymbol{\nabla} + m + \not{v}_{\mathrm{ext}}(\mathbf{x}) + \not{v}_{\mathrm{Hartree}}(\mathbf{x}) + \not{v}_{\mathrm{xc}}(\mathbf{x})\}\psi_i(\mathbf{x}) = \epsilon_i\psi_i(\mathbf{x})\ . \tag{3.48}$$

The effective potential $\not{v} = \gamma_\mu v^\mu$ corresponds to the Feynman dagger notation, so

$$\not{v}_{\mathrm{Hartree}}(\mathbf{x}) = \gamma_\mu v^\mu_{\mathrm{Hartree}}(\mathbf{x})\ , \tag{3.49}$$

$$\not{v}_{\mathrm{xc}}(\mathbf{x}) = \gamma_\mu v^\mu_{\mathrm{xc}}(\mathbf{x}) = \gamma_\mu \frac{\delta E_{\mathrm{xc}}[j^\mu]}{\delta j_\mu(\mathbf{x})}\ , \tag{3.50}$$

[2] On this subsection units of m = 1 will not be used

which has to be solved self-consistently.
Now, one common approximation that can be applied is the so called "no-sea" approximation where one can neglect all radiative corrections

$$j^{\mu}_{\text{vac}} = T_{s,\text{vac}} = E_{\text{xc,vac}} = 0 \ . \tag{3.51}$$

Also, the most usual situation in electronic structure calculations is the one where the external potential is nothing but electrostatic. Consequently, the effective potentials are also electrostatic, so

$$\{v^{\mu}_{\text{Hartree}}(\mathbf{x})\} = \{v^{\mu}_{\text{Hartree}}(\mathbf{x}), 0\} \ . \tag{3.52}$$

Then, the resulting electrostatic no-sea approximation is the standard version applied in practice, written as

$$\{-\mathrm{i}\boldsymbol{\alpha}\cdot\boldsymbol{\nabla} + m\beta + v_{\text{ext}}(\mathbf{x}) + v_{\text{Hartree}}(\mathbf{x}) + v_{\text{xc}}(\mathbf{x})\}\psi_i(\mathbf{x}) = \epsilon_i\psi_i(\mathbf{x}) \ , \tag{3.53}$$

where the density is written as

$$n(\mathbf{x}) = \sum_{-m<\epsilon_i\leq\epsilon_{\text{F}}} \psi^*_i(\mathbf{x}) \ \psi_i(\mathbf{x}) \ . \tag{3.54}$$

Also the exact current $\mathbf{j}[n]$ is usually replaced by the KS current

$$\mathbf{j}(\mathbf{x}) = \sum_{-m<\epsilon_i\leq\epsilon_{\text{F}}} \psi^*_i(\mathbf{x}) \ \boldsymbol{\alpha} \ \psi_i(\mathbf{x}) \ . \tag{3.55}$$

3.4 Exchange and Correlation Functionals

The crucial quantity in the Kohn-Sham approach is the exchange-correlation energy that is expressed as a functional of the density $E_{\text{xc}}[n]$ since the exact functional is not known and it will be necessary to approximate it. Two approaches will be taken into account in this work since they are commonly used: The local spin density approximation (LSDA) and the generalized gradient approximation (GGA).

3.4.1 Local Spin Density Approximation

The LSD is an approximation that was proposed in order to simply consider the local effects of exchange and correlation. Since certain solids can be treated as close to the limit of the homogeneous electron gas, it should be valid when the length scale of the density variation is large in comparison with length scales set by the local density. Also, there are regions of space where LSD is expected to be least reliable, such as near a nucleus or in the evanescent tail of the electron density.

Then, the exchange-correlation energy is an integral over all space with its density at each point assumed to be the same as in homogeneous electron gas:

$$E_{\mathrm{xc}}^{\mathrm{LSDA}}[n^{\uparrow}, n^{\downarrow}] = \int \mathrm{d}\mathbf{r}\; n(\mathbf{r})\; \epsilon_{\mathrm{xc}}^{\mathrm{hom}}(n^{\uparrow}(\mathbf{r}), n^{\downarrow}(\mathbf{r}))\;. \tag{3.56}$$

The exchange-correlation energy per electron of the homogeneous electron gas $\epsilon_{\mathrm{xc}}^{\mathrm{hom}}$ can be written as the sum of exchange energy with correlation energy

$$\epsilon_{\mathrm{xc}}^{\mathrm{hom}}(n^{\uparrow}(\mathbf{r}), n^{\downarrow}(\mathbf{r})) = \epsilon_{\mathrm{x}}^{\mathrm{hom}}(n^{\uparrow}(\mathbf{r}), n^{\downarrow}(\mathbf{r})) + \epsilon_{\mathrm{c}}^{\mathrm{hom}}(n^{\uparrow}(\mathbf{r}), n^{\downarrow}(\mathbf{r}))\;. \tag{3.57}$$

Also, the LSDA can be formulated in terms of either two spin densities $n^{\uparrow}(\mathbf{r})$ and $n^{\downarrow}(\mathbf{r})$ or the total density $n(\mathbf{r})$ and the fractional spin polarization $\xi(\mathbf{r})$ defined as

$$\xi(\mathbf{r}) = \frac{n^{\uparrow}(\mathbf{r}) - n^{\downarrow}(\mathbf{r})}{n(\mathbf{r})}\;. \tag{3.58}$$

For unpolarized systems, $n^{\uparrow}(\mathbf{r})$ and $n^{\downarrow}(\mathbf{r})$ can be set as $n^{\uparrow}(\mathbf{r}) = n^{\downarrow}(\mathbf{r}) = \frac{n(\mathbf{r})}{2}$.

When the LSD approximation is made, the rest is trivial. Also, the exchange energy of the homogeneous gas can be solved analytically and the correlation energy can be found with great accuracy with Monte Carlo methods.

Now, in order to obtain the exchange and correlation potential, we do a functional derivative of E_{xc}

$$V_{\mathrm{xc}}^{\sigma}(\mathbf{r}) = \epsilon_{\mathrm{xc}}([n], \mathbf{r}) + n(\mathbf{r})\frac{\delta\epsilon_{\mathrm{xc}}([n], \mathbf{r})}{\delta n(\mathbf{r}, \sigma)}\;. \tag{3.59}$$

Since in LSDA, δE_{xc} is given by

$$\delta E_{\mathrm{xc}}[n] = \sum_{\sigma} \int \mathrm{d}\mathbf{r} \ \left[\epsilon_{\mathrm{xc}}^{\mathrm{hom}} + n \frac{\partial \epsilon_{\mathrm{xc}}^{\mathrm{hom}}}{\partial n^{\sigma}} \right]_{\mathbf{r},\sigma} \delta n(\mathbf{r}, \sigma) \ , \tag{3.60}$$

the LSDA exchange and correlation potential is

$$V_{\mathrm{xc}}^{\sigma}(\mathbf{r}) = \left[\epsilon_{\mathrm{xc}}^{\mathrm{hom}} + n \frac{\partial \epsilon_{\mathrm{xc}}^{\mathrm{hom}}}{\partial n^{\sigma}} \right]_{\mathbf{r},\sigma} \ . \tag{3.61}$$

3.4.2 Generalized-Gradient Approximation

The success of LSDA stimulated ideas for constructing improved functionals. The first step towards the improvement was to create a functional of the magnitude of the gradient of the density $|\nabla n^{\sigma}|$ as well as the value at each point, it was called "gradient expansion approximation" (GEA), in which the low-order expansion of the exchange and correlation energies is known.
However, the GEA violates the sum rules and other relevant rules. The basic problem is that gradients in real materials are so large that the expansion breaks down and as a result, it leads to a worse precision when comparing to the LSDA. Nonetheless, it also led to the creation of *generalized-gradient approximation* (GGA).
GGA consists on an expansion of the gradients in a variety of ways proposed for functions that modify the behavior at large gradients in such a way as to preserve desired properties. The functional defined at (3.56) is redefined into a generalized form

$$E_{\mathrm{xc}}^{\mathrm{GGA}}[n^{\uparrow}, n^{\downarrow}] = \int \mathrm{d}\mathbf{r} \ n(\mathbf{r}) \ \epsilon_{\mathrm{xc}}(n^{\uparrow}, n^{\downarrow}, |\nabla n^{\uparrow}|, |\nabla n^{\downarrow}|, ...) \ , \tag{3.62}$$

where ϵ_{xc} is redefined as

$$\epsilon_{\mathrm{xc}}(n^{\uparrow}, n^{\downarrow}, |\nabla n^{\uparrow}|, |\nabla n^{\downarrow}|, ...) = \epsilon_{\mathrm{x}}^{\mathrm{hom}}(n) F_{\mathrm{xc}}(n^{\uparrow}, n^{\downarrow}, |\nabla n^{\uparrow}|, |\nabla n^{\downarrow}|, ...) \ , \tag{3.63}$$

with F_{xc} being dimensionless and $\epsilon_{\mathrm{x}}^{\mathrm{hom}}(n)$ being the exchange energy of the unpolarized gas.

Now in the same way that the exchange and correlation potential was obtained on the previous subsection, we do a functional derivative as it was shown on (3.59). The difference is that the GGA δE_{xc} is given by

$$\delta E_{\mathrm{xc}}[n] = \sum_{\sigma} \int \mathrm{d}\mathbf{r} \ \left[\epsilon_{\mathrm{xc}} + n \frac{\partial \epsilon_{\mathrm{xc}}}{\partial n^{\sigma}} + n \frac{\partial \epsilon_{\mathrm{xc}}}{\partial \boldsymbol{\nabla} n^{\sigma}} \boldsymbol{\nabla} \right]_{\mathbf{r},\sigma} \delta n(\mathbf{r}, \sigma) \ . \tag{3.64}$$

Doing the functional partial integration, one may find

$$V_{\mathrm{xc}}^{\sigma}(\mathbf{r}) = \left[\epsilon_{\mathrm{xc}} + n\frac{\partial \epsilon_{\mathrm{xc}}}{\partial n^{\sigma}} - \boldsymbol{\nabla}\left(n\frac{\partial \epsilon_{\mathrm{xc}}}{\partial \boldsymbol{\nabla} n^{\sigma}}\right)\right]_{\mathbf{r},\sigma} . \tag{3.65}$$

3.4.2.1 Explicit PBE form

The PBE form of the GGA functional was developed by Perdew, Burkle and Ezerhof. Here the factor F_x is chosen in a way that the local approximation is recovered by defining $F_x(0) = 1$, and $F_x \rightarrow$ constant at large s, so

$$F_x(s) = 1 + k - \frac{k}{1 + \frac{\mu s^2}{k}} , \tag{3.66}$$

where $k = 0.804$, is a constant defined in order to satisfy the Lieb-Oxford bound, which provides a strict upper bound on the magnitude of the exchange-correlation energy. The constant of $\mu = 0.21951$ is chosen to cancel the term from the correlation.

The local correlation plus an addictive term both of which depending upon the gradients and the spin-polarization, will lead to a form for the correlation energy

$$E_c^{\mathrm{GGA-PBE}}[n^{\uparrow}, n^{\downarrow}] = \int \mathrm{d}\mathbf{r}\; n\left[\epsilon_c^{\mathrm{hom}}(r_s, \xi) + H(r_s, \xi, t)\right] , \tag{3.67}$$

with ξ defined on (3.58) being the spin polarization, r_s is a local value of the density parameter and t is a dimensionless gradient

$$t = \frac{|\nabla n|}{2\phi k_{\mathrm{TF}} n} , \tag{3.68}$$

with ϕ being

$$\phi = \frac{(1+\xi)^{2/3} + (1-\xi)^{2/3}}{2} . \tag{3.69}$$

Also, t is scaled by the screening wavefactor k_{TF} rather than k_{F}, giving

$$H = \frac{\mathrm{e}^2}{a_0}\gamma\phi^3 \log\left(1 + \frac{\beta}{\gamma}t^2\frac{1 + At^2}{1 + At^2 + A^2t^4}\right) , \tag{3.70}$$

with the function A given by

$$A = \frac{\beta}{\gamma} \frac{1}{e^{\frac{-\epsilon_c^{\text{hom}}}{\gamma\phi^3 \frac{e^2}{a_0}}} - 1} \ . \tag{3.71}$$

3.4.3 Non-collinear Spin Density

In the case in which the system exhibits a polarized collinear spin, we can define the system by two different densities and potentials $[n^{\uparrow}(\mathbf{r}), n^{\downarrow}(\mathbf{r})]$ and $[V_{\text{xc}}^{\uparrow}(\mathbf{r}), V_{\text{xc}}^{\downarrow}(\mathbf{r})]$, for spin up and down respectively. However, since spin can vary in space, this is not the most general form. So in the non-collinear spin case, the density is represented by a local spin density matrix

$$\rho^{\alpha\beta}(\mathbf{r}) = \sum_i f_i \ \psi_i^{\alpha *}(\mathbf{r}) \ \psi_i^{\beta}(\mathbf{r}) \ . \tag{3.72}$$

Consequently, the Hamiltonian (3.32) will turn into a 2×2 matrix

$$H_{\text{KS}}^{\alpha\beta}(\mathbf{r}) = -\frac{1}{2}\nabla^2 + V_{\text{KS}}^{\alpha\beta}(\mathbf{r}) \ , \tag{3.73}$$

where the non diagonal part in $\alpha\beta$ of $V_{\text{KS}}^{\alpha\beta}$ is $V_{\text{xc}}^{\alpha\beta}$.
In the local approximation, the functional $\epsilon_{\text{xc}}^{\alpha\beta}$ is given by finding the local axis of spin quantization, using the same functional form $\epsilon_{\text{xc}}^{\text{hom}}(n^{\uparrow}(\mathbf{r}), n^{\downarrow}(\mathbf{r}))$ given in (3.56) . If we want modifications of GGA expressions, we need to take into account the gradient of the spin axis. For further information on Density Functional Theory, check [3], [35], [33] and [32].

Chapter 4

Time-Dependent Density Functional Theory

4.1 Introduction to TDDFT

The *Kohn-Sham ansatz* replaces the many-body problem with an independent-particle problem in which the effective potential depends on the density. Although it envolves independent particles, the density used is the same density of a system of interacting particles. Since the eigenvalues of the KS equations are independent-particle ones that do not correspond to true electron removal or addition energies then, the eigenvalue difference will not consequently correspond to excitation energies. These will be described using response functions that is the response of the system with an external perturbation.

4.2 The Runge-Gross Theorem

The evolution of the N electrons wavefunction is governed by the time-dependent Schrödinger equation (2.27). This is a first-order differential equation in time and so, the initial wavefunction $\Psi(0)$ must be specified. Also $\hat{H}$ is the Hamiltonian operator that can be written as the sum of every other operators acting on the system

$$\hat{H}(\underline{\mathbf{r}}, t) = \hat{T}(\underline{\mathbf{r}}) + \hat{V}_{\text{ee}}(\underline{\mathbf{r}}) + \hat{V}_{\text{ext}}(\underline{\mathbf{r}}, t) \ , \tag{4.1}$$

with coordinates $\underline{\mathbf{r}} = (\mathbf{r}_1, \mathbf{r}_2, ..., \mathbf{r}_N)$. The first term is the kinetic energy of the electrons

$$\hat{T}(\underline{\mathbf{r}}) = -\frac{1}{2}\sum_{i=1}^{N}\nabla_i^2 \ , \tag{4.2}$$

and $\hat{V}_{\mathrm{ee}}(\underline{\mathbf{r}})$ is the Coulomb electron-electron repulsion

$$\hat{V}_{\mathrm{ee}}(\underline{\mathbf{r}}) = \frac{1}{2}\sum_{i\neq j}^{N}\frac{1}{|\mathbf{r}_i - \mathbf{r}_j|} \ . \tag{4.3}$$

The external potential $\hat{V}_{\mathrm{ext}}(\underline{\mathbf{r}}, t)$ is a generic, time-dependent potential that affects electrons. Also, the one-body potential is written as

$$\hat{V}_{\mathrm{ext}}(\underline{\mathbf{r}}, t) = \sum_{i=1}^{N} v_{\mathrm{ext}}(\mathbf{r}_i, t) \ . \tag{4.4}$$

For a hydrogenic atom with nuclear charge Z in an alternating electric field of strength $\boldsymbol{\varepsilon}$ oriented along the z axis and of frequency ω we have $v_{\mathrm{ext}}(\underline{\mathbf{r}}, t) = -Z/r + \boldsymbol{\varepsilon}\cdot z\cos(\omega, t)$. However it is the only operator that differs from problem to problem.

Now, the Runge-Gross theorem is an extension of the HK theorems for time-dependent problems. Let us start with the ground-state of the system that can be determined through the minimization of the total energy functional

$$E[\Phi] = \left\langle \Phi \middle| \hat{H} \middle| \Phi \right\rangle \ . \tag{4.5}$$

However, in time-dependent systems, since the basis of the total energy is not a conserved quantity, then there is no variational principle. A way to avoid this problem is to use the quantum mechanical action, that is a quantity similar to the energy

$$\mathcal{A}[\Phi] = \int_{t_0}^{t_1} \mathrm{dt} \ \left\langle \Phi(t) \middle| \mathrm{i}\frac{\partial}{\partial t} - \hat{H}(t) \middle| \Phi(t) \right\rangle \ , \tag{4.6}$$

where $\Phi(t)$ is a N-body function defined in some convenient space. As we can notice, if we take the functional derivative to zero in terms of $\psi^*(t)$, we obtain the time-dependent Schrödinger equation. Therefore we can solve the time-dependent problem by calculating the stationary point of the functional $\mathcal{A}[\psi]$. The function $\Psi(t)$ that makes the functional stationary, $\mathcal{A}[\psi] = 0$, will be the many-body time-dependent Schrödinger equation solution. Now, since it is already known that the RG theorem is a bit more complicated and

subtle that the KS ones, even though the first is pretty much the time-dependent extension of the second one, let us demonstrate that having two different potentials $v_{\text{ext}}^{(1)}(\mathrm{r},t)$ and $v_{\text{ext}}^{(2)}(\mathrm{r},t)$, that differs by more that a purely time-dependent function $c(t)$, i.e. their wavefunctions shift by more than a mere time-dependent phase and, as a consequence, there will be different time-dependent densities

$$v_{\text{ext}}^{(1)}(\mathrm{r},t) \neq v_{\text{ext}}^{(2)}(\mathrm{r},t) + c(t) \Rightarrow n^{(1)}(\mathbf{r},t) \neq n^{(2)}(\mathbf{r},t)\ . \tag{4.7}$$

This implies that for each potential there is a correspondent time-dependent density. Now lets assume that the external potentials are Taylor expandable with respect to the time coordinate around the initial time t_0

$$v_{\text{ext}}(\mathbf{r},t) = \sum_{k=0}^{\infty} c_k(\mathbf{r})(t-t_0)^k, \tag{4.8}$$

with $c_k(\mathbf{r})$ being the expansion coefficient of index k

$$c_k(\mathbf{r}) = \frac{1}{k!}\frac{\partial^k}{\partial t^k} v_{\text{ext}}(\mathbf{r},t)\bigg|_{t=t_0}\ . \tag{4.9}$$

Also, a function will be defined as

$$u_k(\mathbf{r}) = \frac{\partial^k}{\partial t^k}[v_{\text{ext}}^{(1)}(\mathbf{r},t) - v_{\text{ext}}^{(2)}(\mathbf{r},t)]\bigg|_{t=t_0}\ . \tag{4.10}$$

Since two different potentials are different by more than a td function, then at least one expansion coefficient will differ by more than a constant. So, the first step is to show that if $v_{\text{ext}}^{(1)} \neq v_{\text{ext}}^{(2)} + c(t)$, then the current densities, $\mathbf{j}^{(1)}$ and $\mathbf{j}^{(2)}$ given by $v_{\text{ext}}^{(1)}$ and $v_{\text{ext}}^{(2)}$ are also different. The current density can be written as the expectation value of the current density operator

$$\mathbf{j}(\mathbf{r},t) = \left\langle \Psi(t)\middle|\hat{\mathbf{j}}(\mathbf{r})\middle|\Psi(t)\right\rangle\ . \tag{4.11}$$

with the operator $\hat{\mathbf{j}}$ being

$$\hat{\mathbf{j}}(\mathbf{r}) = -\frac{1}{2\mathrm{i}}\left\{ \left[\nabla\hat{\psi}^*(\mathbf{r})\right]\hat{\psi}(\mathbf{r}) - \hat{\psi}^*(\mathbf{r})\left[\nabla\hat{\psi}(\mathbf{r})\right]\right\}\ . \tag{4.12}$$

If we use now the quantum-mechanical equation of motion valid for any operator $\hat{O}$ then

$$\mathrm{i}\frac{d}{dt}\big\langle\Psi(t)\big|\hat{O}(t)\big|\Psi(t)\big\rangle = \big\langle\Psi(t)\big|\mathrm{i}\frac{\partial}{\partial t}\hat{O}(t) + \Big[\hat{O}(t),\hat{H}(t)\Big]\big|\Psi(t)\big\rangle \ . \tag{4.13}$$

Writing now the equation of motion for 2 different current densities produced by $v_{\mathrm{ext}}^{(1)}$ and $v_{\mathrm{ext}}^{(2)}$, noting that the operator $\hat{\mathbf{j}}$ is not time-dependent and so $\mathrm{i}\frac{\partial}{\partial t}\hat{\mathbf{j}} = 0$, we get

$$\mathrm{i}\frac{d}{dt}\mathbf{j}^{(1)}(\mathbf{r},t) = \big\langle\Psi(t)\big|\Big[\hat{\mathbf{j}}(\mathbf{r}),\hat{H}^{(1)}(t)\Big]\big|\Psi(t)\big\rangle \ , \tag{4.14}$$

$$\mathrm{i}\frac{d}{dt}\mathbf{j}^{(2)}(\mathbf{r},t) = \big\langle\Psi(t)\big|\Big[\hat{\mathbf{j}}(\mathbf{r}),\hat{H}^{(2)}(t)\Big]\big|\Psi(t)\big\rangle \ . \tag{4.15}$$

Starting from a fixed many-body state, at t_0, the wavefunctions, densities and current densities are written as

$$\big|\Psi^{(1)}(t_0)\big\rangle = \big|\Psi^{(2)}(t_0)\big\rangle = \big|\Psi_0(t_0)\big\rangle \ , \tag{4.16}$$

$$n^{(1)}(\mathbf{r},t_0) = n^{(2)}(\mathbf{r},t_0) = n_0(\mathbf{r}) \ , \tag{4.17}$$

$$\mathbf{j}^{(1)}(\mathbf{r},t_0) = \mathbf{j}^{(2)}(\mathbf{r},t_0) = \mathbf{j}_0(\mathbf{r}) \ . \tag{4.18}$$

Taking now the differences between the equations of motion (4.14) and (4.15) at $t = t_0$, we get

$$\mathrm{i}\frac{\mathrm{d}}{\mathrm{d}t}\Big[\mathbf{j}^{(1)}(\mathbf{r},t) - \mathbf{j}^{(2)}(\mathbf{r},t)\Big]_{t=t_0} = \big\langle\Psi_0\big|\Big[\hat{\mathbf{j}}(\mathbf{r}),\hat{H}^{(1)}(t_0) - \hat{H}^{(2)}(t_0)\Big]\big|\Psi_0\big\rangle \ , \tag{4.19}$$

$$\big\langle\Psi_0\big|\Big[\hat{\mathbf{j}}(\mathbf{r}),\hat{H}^{(1)}(t_0) - \hat{H}^{(2)}(t_0)\Big]\big|\Psi_0\big\rangle = \big\langle\Psi_0\big|\Big[\hat{\mathbf{j}}(\mathbf{r}),v_{\mathrm{ext}}^{(1)}(\mathbf{r},t_0) - v_{\mathrm{ext}}^{(2)}(\mathbf{r},t_0)\Big]\big|\Psi_0\big\rangle \ , \tag{4.20}$$

$$\big\langle\Psi_0\big|\Big[\hat{\mathbf{j}}(\mathbf{r}),v_{\mathrm{ext}}^{(1)}(\mathbf{r},t_0) - v_{\mathrm{ext}}^{(2)}(\mathbf{r},t_0)\Big]\big|\Psi_0\big\rangle = \mathrm{i}\ n_0(\mathbf{r})\nabla\Big[v_{\mathrm{ext}}^{(1)}(\mathbf{r},t_0) - v_{\mathrm{ext}}^{(2)}(\mathbf{r},t_0)\Big] \ . \tag{4.21}$$

Assuming that for $k = 0$, $v_{\text{ext}}^{(1)} \neq v_{\text{ext}}^{(2)}$ at $t = t_0$, implying that the left side of equation (4.19) differs from zero, then the two currents $\mathbf{j}^{(1)}$ and $\mathbf{j}^{(2)}$ will drift for $t > t_0$. Now for k greater than zero, the equation of motion is applied $k + 1$ times, which yields

$$\frac{\mathrm{d}^{k+1}}{\mathrm{d}t^{k+1}} \left[\mathbf{j}^{(1)}(\mathbf{r}, t) - \mathbf{j}^{(2)}(\mathbf{r}, t)\right]_{t=t_0} = n_0(\mathbf{r})\nabla u_k(\mathbf{r}) \ , \tag{4.22}$$

with u_k defined previously in equation (4.10). Since there are values of k where its derivative differs from 0, then $\mathbf{j}^{(1)}(\mathbf{r}, t) \neq \mathbf{j}^{(2)}(\mathbf{r}, t)$ at $t > t_0$, bringing to a closure the proof for the first step of the theorem.

Now, the second step consists on proving that $\mathbf{j}^{(1)} \neq \mathbf{j}^{(2)}$ implies $n^{(1)} \neq n^{(2)}$. In order to prove that, we may bring into play the continuity equation

$$\frac{\partial}{\partial t} n(\mathbf{r}, t) = -\nabla \cdot \mathbf{j}(\mathbf{r}, t) \ . \tag{4.23}$$

Taking then the difference between the two systems (1) and (2), we get

$$\frac{\partial}{\partial t} \left[n^{(1)}(\mathbf{r}, t) - n^{(2)}(\mathbf{r}, t)\right] = -\nabla \cdot \left[\mathbf{j}^{(1)}(\mathbf{r}, t) - \mathbf{j}^{(2)}(\mathbf{r}, t)\right] \ . \tag{4.24}$$

We will apply the $(k + 1)$th time-derivative at $t = t_0$ on the previous equation in order to get kth time derivative, i.e. using the same reasoning from equation (4.22)

$$\begin{aligned} \frac{\partial^{k+2}}{\partial t^{k+2}} \left[n^{(1)}(\mathbf{r}, t) - n^{(2)}(\mathbf{r}, t)\right]_{t=t_0} &= -\nabla \cdot \frac{\partial^{k+1}}{\partial t^{k+1}} \left[\mathbf{j}^{(1)}(\mathbf{r}, t) - \mathbf{j}^{(2)}(\mathbf{r}, t)\right]_{t=t_0} \ . \\ &= -\nabla \cdot [n_0(\mathbf{r})\nabla u_k(\mathbf{r})] \end{aligned} \tag{4.25}$$

From the implication of equation (4.22), it was made clear that

$$\nabla \cdot [n_0(\mathbf{r})\nabla u_k(\mathbf{r})] \neq 0 \ , \tag{4.26}$$

and, as a result, $n^{(1)} \neq n^{(2)}$, proving then the last step of the Runge-Gross theorem.

4.3 Time-Dependent Kohn-Sham Equations

It is rather difficult to find functionals, in particular the kinetic energy, as an explicit functional of the density. However, just as in the ground-state theory, we turn to a non-interacting system of fermions called the Kohn-Sham system, defined such as in section (3.3), reproducing the density of the true interacting system, so all properties can be extracted from the density of the KS system. Also, the KS potential is unique by virtue of the Runge-Gross theorem applied to the non-interacting system, and is chosen such as the density of the KS electrons is the same as the density of the original interacting system. So, these KS electrons obey to the time-dependent Schrödinger equation

$$\mathrm{i}\frac{\partial}{\partial t}\varphi_i(\mathbf{r},t) = \left[-\frac{\nabla^2}{2} + v_{\mathrm{KS}}[n,\Phi_0](\mathbf{r},t)\right]\varphi_i(\mathbf{r},t)\ , \tag{4.27}$$

where Φ_0 represent the initial state of the Kohn-Sham system and $\varphi_i(\mathbf{r},t)$ are orbitals that satisfy the previous equation. Also, the density of the interacting system can be obtained from the time-dependent Kohn-Sham orbitals

$$n(\mathbf{r},t) = \sum_{i=1}^{N} \varphi_i^*(\mathbf{r},t)\varphi_i(\mathbf{r},t)\ . \tag{4.28}$$

Analogously to the ground-state case, v_{KS} is decomposed into three terms

$$v_{KS}[n,\Phi_0](\mathbf{r},t) = v_{\mathrm{ext}}[n,\Psi_0](\mathbf{r},t) + v_{\mathrm{Hartree}}[n](\mathbf{r},t) + v_{\mathrm{xc}}[n,\Psi_0,\Phi_0](\mathbf{r},t)\ . \tag{4.29}$$

The first term $v_{\mathrm{ext}}[n,\Psi_0](\mathbf{r},t)$ represents the external time-dependent field, the second is the Hartree potential, which describes the interaction of classical electronic charge distribution

$$v_{\mathrm{Hartree}}[n](\mathbf{r},t) = \int \mathrm{d}\mathbf{r}_2\ \frac{n(\mathbf{r}_2,t)}{|\mathbf{r}_1-\mathbf{r}_2|}\ . \tag{4.30}$$

At last, the third term represents the exchange and correlation potential, which comprises all the non-trivial many-body effects. Normally, it is written as a functional derivative of the exchange and correlation energy, that follows from a variational derivation of the Kohn-Sham equations starting from the total energy. However, for the time-dependent case it was necessary to define a new action functional $\tilde{\mathcal{A}}$ by the Keldish formalism due to causality problems. The time-dependent xc potential will then be written as the functional derivative of the xc part of $\tilde{\mathcal{A}}$

$$v_{\mathrm{xc}}(\mathbf{r},t) = \left.\frac{\partial \tilde{\mathcal{A}}_{\mathrm{xc}}}{\partial n(\mathbf{r},\tau)}\right|_{n(\mathbf{r},t)} , \tag{4.31}$$

where τ stands for the Keldish pseudo-time. Since the exact expression of v_{xc} as a functional of the density is unknown, then an approximation is necessary to do. The simplest to be done is the ALDA, which stands for Adiabatic local density approximation.

4.3.1 Adiabatic approximation

On the previous chapter, it was mentioned that the exchange and correlation potential v_{xc} is a functional with a dependence on the density $n(\mathbf{r},t)$ for a given $\mathbf{r}$ and t. However, it has also a dependence on all $n(\mathbf{r},t')$ for $0 \leq t' \leq t$ and for arbitrary points $\mathbf{r}'$, so we may say that the potential has memory since it remembers its past density.

So, the adiabatic approximation consists on ignoring all the past densities and allow only the instantaneous ones. In other words, the functional can be approximated as being local in time

$$v_{\mathrm{xc}}^{\mathrm{adia}}[n](\mathbf{r},t) = \tilde{v}_{\mathrm{xc}}[n](\mathbf{r})|_{n=n(t)} , \tag{4.32}$$

where $\tilde{v}_{\mathrm{xc}}[n]$ is assumed to be an approximation to the ground-state exchange and correlation density functional. This approximation will be valid if the time-dependent potential changes very slowly, i.e. , we have an adiabatic process.

Since the exact exchange and correlation energy functional is not known, even in the static case, then we shall insert the LDA functional mentioned in 3.4.1 on equation (4.32) to obtain the *Adiabatic Local Density Approximation* (ALDA). The same method can be applied in order to get the AGGA, however further results have shown that there is no big difference between both of them.

4.4 Linear Response Theory

The main goal of this section is to show that for an arbitrary external field acting on a sample, there will be a response from that sample that can be measured for some physical observable $\mathcal{P}$ that is dependent on the function F

$$\Delta\mathcal{P} = \Delta\mathcal{P}_F[F] . \tag{4.33}$$

The function of the observable must produce a response for any created field, i.e. weak or strong, so the response can be expanded as a power series with respect to field strength. However, since we are interested on weak electric perturbations, we can ignore higher order response and focus on first-order ones, also known as linear-response of the observable given by

$$\delta\mathcal{P}^{(1)}(\mathbf{r},t) = \int \mathrm{d}t_1 \int \mathrm{d}\mathbf{r}_2 \; \chi^{(1)}_{\mathcal{P}\leftarrow F}(\mathbf{r}_1,\mathbf{r}_2,t_1-t_2)\delta F^{(1)}(\mathbf{r}_2,t_2) \; , \tag{4.34}$$

with $\delta\mathcal{P}^{(1)}(\mathbf{r},t)$ being a convolution of the linear response function $\chi^{(1)}_{\mathcal{P}\leftarrow F}(\mathbf{r}_1,\mathbf{r}_2,t_1-t_2)$ and the field expanded to the first order in field strength $\delta F(\mathbf{r}_2,t_2)$. Although the linear response function is nonlocal in space and time, the time convolution is simplified into a product in frequency space

$$\delta\mathcal{P}^{(1)}(\mathbf{r},\omega) = \int \mathrm{d}\mathbf{r}_2 \; \chi^{(1)}_{\mathcal{P}\leftarrow F}(\mathbf{r}_1,\mathbf{r}_2,\omega)\delta F^{(1)}(\mathbf{r}_2,\omega) \; . \tag{4.35}$$

Since time is homogeneous, the linear response function depends only on the frequency ω. So, the linear density response in the frequency space will be given as

$$\delta n(\mathbf{r},\omega) = \int \mathrm{d}\mathbf{r}_2 \; \chi_{\mathrm{KS}}(\mathbf{r}_1,\mathbf{r}_2,\omega)\delta v_{\mathrm{KS}}(\mathbf{r}_2,\omega) \; . \tag{4.36}$$

4.4.1 Dynamic polarizability tensor

There are several methods to calculate response functions, the most known ones are the time-propagation, Sternheimer and Casida. The Sternheimer method consists on perturbing the system with respect to λ, which is the perturbation strength. The Casida method takes the linear Sternheimer equation in the KS orbital basis, including unoccupied states. The approach that will be used in this work is the time-propagation method, which consists of three main steps. The first one is to get the ground-state occupied wavefunctions. Then the ground-state is perturbed by multiplying each of the single-particle KS wavefunction by a phase $\mathrm{e}^{-\mathrm{i}(\mathbf{r}\cdot\mathcal{E})}$, which shifts the momentum of the electrons. In order to study the linear dipole response, the strength of the applied homogeneous electric field must be much smaller than the inverse radius of the system. At last, the system is then propagated until some finite time T. The time-dependent Kohn-Sham equations are propagated in real time by solving the nonlinear partial equation

$$\mathrm{i}\frac{\partial}{\partial t}\varphi_k(\mathbf{r},t) = \hat{H}_{\mathrm{KS}}[n](\mathbf{r},t)\varphi_k(\mathbf{r},t) \; , \tag{4.37}$$

starting from $t = 0$ with the initial conditions $\varphi(\mathbf{r}, t = 0) = \varphi_k^{(0)}(\mathbf{r})$ where $\varphi_k^{(0)}(\mathbf{r})$ are the ground-state KS wavefunctions. The time-evolution of the KS wavefunctions, if no perturbation is applied to the system, is $\varphi_k(t) = \varphi^{(0)} \mathrm{e}^{-\mathrm{i}\varepsilon_k^{(0)} t}$. Applying then a weak time-dependent external perturbation with a given frequency ω defined in the following general form

$$v_{\mathrm{ext}}(\mathbf{r}, t) = \lambda v_{\mathrm{ext}}^{\cos}(\mathbf{r}) \cos \omega t + \lambda v_{\mathrm{ext}}^{\sin}(\mathbf{r}) \sin \omega t \ , \tag{4.38}$$

or, in the exponential form

$$v_{\mathrm{ext}}(\mathbf{r}, t) = \lambda v_{\mathrm{ext}}^{+\omega}(\mathbf{r}) \mathrm{e}^{+\mathrm{i}\omega t} + \lambda v_{\mathrm{ext}}^{-\omega}(\mathbf{r}) \mathrm{e}^{-\mathrm{i}\omega t} \ , \tag{4.39}$$

with λ being the strength of the perturbation. Applying then a weak delta pulse of a dipole electric field

$$v_{\mathrm{ext}}(\mathbf{r}, t) = \mathbf{r} \cdot \mathcal{E} \ \delta(t) = \mathbf{r} \cdot \mathcal{E} \ \frac{1}{2\pi} \int_{-\infty}^{\infty} \mathrm{d}\omega \ \mathrm{e}^{\mathrm{i}\omega t} \ . \tag{4.40}$$

Now, we can replace the ground-state wavefunctions by

$$\begin{aligned} \varphi_k(\mathbf{r}, t = 0^+) &= \mathrm{e}^{-\mathrm{i} \int_{0^-}^{0^+} \mathrm{d}t \left[\hat{H}_{\mathrm{KS}}^{(0)}(t) + \mathbf{r} \cdot \mathcal{E} \ \delta(t) \right]} \varphi_k(\mathbf{r}, t = 0^-) \ , \\ &= \mathrm{e}^{-\mathrm{i}(\mathbf{r} \cdot \mathcal{E})} \varphi_k(\mathbf{r}, t = 0^-) \end{aligned} \tag{4.41}$$

with $\mathrm{e}^{-\mathrm{i}(\mathbf{r} \cdot \mathcal{E})}$ being the "kick" that the wavefunction suffers, or the phase shift as was mentioned earlier. Now we can propagate the free oscillations in time. Also, the time-dependent dipole moment can be written as

$$\boldsymbol{\mu}(t) = \int \mathrm{d}\mathbf{r} \ \mathbf{r} \ n(\mathbf{r}, t) \ . \tag{4.42}$$

Now doing the first-order Taylor expansion of the dipole moment

$$\mu_i(\omega) = \mu_{i0} + \alpha_{ij}(\omega) \mathcal{E}_j^{\omega} + \dots \ , \tag{4.43}$$

which means that the linear dynamic polarizability tensor is given by

$$\alpha_{ij}(\omega) = \frac{1}{\mathcal{E}_j^{\omega}}(\mu_i(\omega) - \mu_{i0}) \ . \tag{4.44}$$

If the perturbing field is small enough, the difference between the dipole moments can be approximated as an infinitesimal dipole moment

$$\alpha_{ij}(\omega) = \frac{1}{\mathcal{E}_j^{\omega}}\delta\mu(\omega) \ . \tag{4.45}$$

Writing the equation (4.42) on the infinitesimal form and on the frequency space, we get

$$\delta\mu(\omega) = \int \mathrm{d}\mathbf{r}\ \mathbf{r}\ \delta n(\mathbf{r},\omega) \ , \tag{4.46}$$

with $\delta n(\mathbf{r},\omega)$ defined on (4.36). The previous equation can be rewritten as

$$\delta\mu(\omega) = \int \mathrm{d}\mathbf{r}_1\ \mathbf{r}_1 \int \mathrm{d}\mathbf{r}_2\ \chi(\mathbf{r}_1,\mathbf{r}_2,\omega)\delta v(\mathbf{r}_2,\omega) \ , \tag{4.47}$$

and, from equation (4.45) we obtain the dynamic polarizability tensor

$$\alpha_{ij}(\omega) = \frac{1}{\mathcal{E}_j^{\omega}} \int \mathrm{d}\mathbf{r}_1\ r_{1,i} \int \mathrm{d}\mathbf{r}_2\ \chi(\mathbf{r}_1,\mathbf{r}_2,\omega)\delta v_{\mathrm{ext}}(\mathbf{r}_2,\omega) \ , \tag{4.48}$$

with δv_{ext} being the perturbed potential and χ the density response function. Since $\delta v_{\mathrm{ext}} = -\mathbf{r}\cdot\mathcal{E} = -r_j\mathcal{E}_j^{\omega}$ in a given direction, the polarizability tensor can be written as

$$\alpha_{ij}(\omega) = -\int \mathrm{d}\mathbf{r}_1 \int \mathrm{d}\mathbf{r}_2\ r_{1,i}\ \chi(\mathbf{r}_1,\mathbf{r}_2,\omega)\ r_{2,j} \ , \tag{4.49}$$

where the index $r_{1,i}$ represents one particle on a direction i and $r_{2,j}$ represents other particle on the direction j.

Also, the cross-section for optical absorption can be obtained using the imaginary part of the polarizability resulting in

$$\sigma_{ij}(\omega) = \frac{4\pi\omega}{c}\mathcal{I}m\{\alpha_{ij}(\omega)\} \ . \tag{4.50}$$

Finally, if we want the cross-section averaged over three spatial directions, one writes

$$\sigma = \frac{1}{3}\mathrm{Tr}(\sigma_{ij}) \ . \tag{4.51}$$

This is the quantity that is usually measured in experiments.

4.4.1.1 Spin-dependent polarizability tensor

In the previous subsection it was shown how to reach the spin-independent polarizabilities, but what if, not only the perturbation, but also the observable is spin-dependent? Let us start with a general perturbation $\delta v_\sigma(\mathbf{r},\omega)$ in which σ represents the spin-up $\uparrow$ and spin-down $\downarrow$ electrons. It is also important to notice that $\delta v_\uparrow(\mathbf{r},\omega)$ and $\delta v_\downarrow(\mathbf{r},\omega)$ may be different. So the response functions is given as

$$\delta n_\sigma(\mathbf{r},\omega) = \sum_{\sigma_2} \int \mathrm{d}\mathbf{r}_2 \ \chi_{\sigma_1\sigma_2}(\mathbf{r}_1,\mathbf{r}_2,\omega)\delta v_{\sigma_2}(\mathbf{r}_2,\omega) \ , \tag{4.52}$$

which is called spin-density response function since only the perturbation is spin-dependent, moreover, if the perturbation is spin-independent, it would be called density-density response function $n = n_\uparrow + n_\downarrow$, if only the observable is spin-dependent, would be density-spin response function $m = n_\uparrow - n_\downarrow$, at last, if both are spin-dependent, it would be called spin-spin response function, in other words, it is implied that "spin-spin", "spin-density", "density-spin" and "density-density" are reffering to the perturbed function and to the observable respectively. Now the sum of the spin-up and down densities will give the total density

$$n = n_\uparrow + n_\downarrow \Rightarrow \delta n(\mathbf{r},\omega) = \delta n_\uparrow(\mathbf{r},\omega) + \delta n_\downarrow(\mathbf{r},\omega) \ . \tag{4.53}$$

Also, the magnetization density is given by

$$m = n_\uparrow - n_\downarrow \Rightarrow \delta m(\mathbf{r},\omega) = \delta n_\uparrow(\mathbf{r},\omega) - \delta n_\downarrow(\mathbf{r},\omega) \ . \tag{4.54}$$

As a result, one may write the variation of the time-dependent spin-dipole moment as

$$\boldsymbol{\nu}(t) = \int \mathrm{d}\mathbf{r} \ \mathbf{r} \ m(\mathbf{r},t) \ . \tag{4.55}$$

Considering then two different perturbations

$$\delta v_{\sigma}^{[n]}(\mathbf{r},\omega) = -r_j \mathcal{E}_j^{\omega} \ , \tag{4.56}$$

$$\delta v_{\sigma}^{[m]}(\mathbf{r},\omega) = -r_j \mathcal{E}_j^{\omega} \sigma_z \ . \tag{4.57}$$

If $\sigma =\uparrow$, then $\sigma_z = 1$, also if $\sigma =\downarrow$ then $\sigma_z = -1$, so from (4.57) we obtain

$$\delta v_{\uparrow}^{[m]}(\mathbf{r},\omega) = -r_j \mathcal{E}_j^{\omega} \ , \tag{4.58}$$

$$\delta v_{\downarrow}^{[m]}(\mathbf{r},\omega) = r_j \mathcal{E}_j^{\omega} \ . \tag{4.59}$$

Now, both variations δn and δm, that corresponds to density-density and density-spin response functions respectively, in which we can consequently state that (4.56) is spin-independent and (4.57) is spin-dependent, are given as

$$\begin{aligned}
\delta n^{[n]}(\mathbf{r},\omega) &= -\mathcal{E}_j^{\omega} \int \mathrm{d}\mathbf{r}_2 \ \chi^{[nn]}(\mathbf{r}_1,\mathbf{r}_2,\omega) \ r_{2,j} \\
\delta m^{[n]}(\mathbf{r},\omega) &= -\mathcal{E}_j^{\omega} \int \mathrm{d}\mathbf{r}_2 \ \chi^{[mn]}(\mathbf{r}_1,\mathbf{r}_2,\omega) \ r_{2,j} \\
\delta n^{[n]}(\mathbf{r},\omega) &= -\mathcal{E}_j^{\omega} \int \mathrm{d}\mathbf{r}_2 \ \chi^{[nm]}(\mathbf{r}_1,\mathbf{r}_2,\omega) \ r_{2,j} \\
\delta m^{[n]}(\mathbf{r},\omega) &= -\mathcal{E}_j^{\omega} \int \mathrm{d}\mathbf{r}_2 \ \chi^{[mm]}(\mathbf{r}_1,\mathbf{r}_2,\omega) \ r_{2,j}
\end{aligned} \tag{4.60}$$

Where $[n]$ and $[m]$ represents the spin-independent-like and spin-dependent perturbations on δn and δm. Also, the linear response functions will be defined as

$$\begin{aligned}
\chi^{[nn]} &= \chi_{\uparrow\uparrow} + \chi_{\uparrow\downarrow} + \chi_{\downarrow\uparrow} + \chi_{\downarrow\downarrow} \\
\chi^{[mn]} &= \chi_{\uparrow\uparrow} + \chi_{\uparrow\downarrow} - \chi_{\downarrow\uparrow} - \chi_{\downarrow\downarrow} \\
\chi^{[nm]} &= \chi_{\uparrow\uparrow} - \chi_{\uparrow\downarrow} + \chi_{\downarrow\uparrow} - \chi_{\downarrow\downarrow} \\
\chi^{[mm]} &= \chi_{\uparrow\uparrow} - \chi_{\uparrow\downarrow} - \chi_{\downarrow\uparrow} + \chi_{\downarrow\downarrow}
\end{aligned} \tag{4.61}$$

Having then δn, δm and combining (4.45) with (4.46), we get the following equations as a result

$$\begin{aligned}
\alpha_{ij}^{[nn]}(\omega) &= -\int \mathrm{d}\mathbf{r}_1 \int \mathrm{d}\mathbf{r}_2\ r_{1,i}\ \chi^{[nn]}(\mathbf{r}_1,\mathbf{r}_2,\omega)\ r_{2,j} \\
\alpha_{ij}^{[mn]}(\omega) &= -\int \mathrm{d}\mathbf{r}_1 \int \mathrm{d}\mathbf{r}_2\ r_{1,i}\ \chi^{[mn]}(\mathbf{r}_1,\mathbf{r}_2,\omega)\ r_{2,j} \\
\alpha_{ij}^{[nm]}(\omega) &= -\int \mathrm{d}\mathbf{r}_1 \int \mathrm{d}\mathbf{r}_2\ r_{1,i}\ \chi^{[nm]}(\mathbf{r}_1,\mathbf{r}_2,\omega)\ r_{2,j} \\
\alpha_{ij}^{[mm]}(\omega) &= -\int \mathrm{d}\mathbf{r}_1 \int \mathrm{d}\mathbf{r}_2\ r_{1,i}\ \chi^{[mm]}(\mathbf{r}_1,\mathbf{r}_2,\omega)\ r_{2,j}
\end{aligned} \tag{4.62}$$

It is important to note that the polarizability that is usually mentioned is $\alpha = \alpha_{ij}^{[nn]}$, also, the previous equations can be rewritten as

$$\alpha = \alpha_{ij}^{\sigma_1\sigma_2}(\omega) = -\int \mathrm{d}\mathbf{r}_1 \int \mathrm{d}\mathbf{r}_2\ r_{1,i}\ \chi_{\sigma_1\sigma_2}(\mathbf{r}_1,\mathbf{r_2},\omega)\ r_{2,j}\ . \tag{4.63}$$

Since α is directly related with χ, then equations (4.62) can also be written as

$$\begin{aligned}
\alpha_{ij}^{[nn]} &= \alpha_{ij}^{\uparrow\uparrow} + \alpha_{ij}^{\uparrow\downarrow} + \alpha_{ij}^{\downarrow\uparrow} + \alpha_{ij}^{\downarrow\downarrow} \\
\alpha_{ij}^{[mn]} &= \alpha_{ij}^{\uparrow\uparrow} + \alpha_{ij}^{\uparrow\downarrow} - \alpha_{ij}^{\downarrow\uparrow} - \alpha_{ij}^{\downarrow\downarrow} \\
\alpha_{ij}^{[nm]} &= \alpha_{ij}^{\uparrow\uparrow} - \alpha_{ij}^{\uparrow\downarrow} + \alpha_{ij}^{\downarrow\uparrow} - \alpha_{ij}^{\downarrow\downarrow} \\
\alpha_{ij}^{[mm]} &= \alpha_{ij}^{\uparrow\uparrow} - \alpha_{ij}^{\uparrow\downarrow} - \alpha_{ij}^{\downarrow\uparrow} + \alpha_{ij}^{\downarrow\downarrow}
\end{aligned} \tag{4.64}$$

Where the dipole Strength function and the spin-dipole strength function can be define with the response functions $\alpha_{ij}^{[nn]}$ and $\alpha_{ij}^{[mm]}$ respectively

$$\begin{aligned}
S^{[nn]}(\omega) &= \frac{2\omega}{\pi}\mathcal{I}m\left\{ \mathrm{Tr}\left[\alpha^{[nn]}(\omega)\right] \right\}, \\
S^{[mm]}(\omega) &= \frac{2\omega}{\pi}\mathcal{I}m\left\{ \mathrm{Tr}\left[\alpha^{[mm]}(\omega)\right] \right\}.
\end{aligned} \tag{4.65}$$

Since the dipole strength function is related to $\alpha^{[nn]}$, then it is indeed also related to the optical absorption cross section (4.50) so

$$S(\omega) = \frac{1}{2}\frac{c}{\pi^2}\sigma(\omega)\ . \tag{4.66}$$

With units of $\hbar = m = 1$. Also, the spin-dipole strength function carries information about the spin dipole modes of excitation.

Chapter 5

Pseudopotentials

5.1 The Pseudopotential formulation

The base of the DFT is the many-body approach of a quantum system so, a way to simplify the many-electron Schrödinger equation is to split the electrons of the system into the valence electrons and the inner core electrons. Since the electrons in the inner shell are strongly bound they are in an almost static regime, thus they can generally be ignored, this implies that the atom will have an ionic core interacting with the valence electrons.

In this section, the core electrons will be denoted as $|\psi_c\rangle$ and the valence ones will be $|\psi_v\rangle$, so

$$\hat{H}|\psi_n\rangle = E_n|\psi_n\rangle \ , \tag{5.1}$$

where $n = c, v$. Also, the valence orbitals can be written as the sum of the pseudo wavefunction, which is a smooth function $|\varphi_v\rangle$ with an oscillating function that results from the orthogonalization of the valence to the inner core orbitals

$$|\psi_v\rangle = |\varphi_v\rangle + \sum_c \alpha_{cv}|\psi_c\rangle \ , \tag{5.2}$$

with α_{cv} being $-\langle\psi_c|\varphi_v\rangle$. From (5.1) we get $\hat{H}|\psi_v\rangle = E_v|\psi_v\rangle$ and from (5.2) we get

$$\begin{aligned}\hat{H}\left(|\varphi_v\rangle + \sum_c \alpha_{cv}|\psi_c\rangle\right) &= E_v\left(|\varphi_v\rangle + \sum_c \alpha_{cv}|\psi_c\rangle\right) \Leftrightarrow \\ \hat{H}|\varphi_v\rangle + \sum_c \hat{H}|\psi_c\rangle\alpha_{cv} &= E_v|\varphi_v\rangle + E_v\sum_c \alpha_{cv}|\psi_c\rangle \ .\end{aligned} \tag{5.3}$$

Once again, from (5.1), one can obtain

$$\sum_c \hat{H}|\psi_c\rangle\alpha_{cv} = \sum_c E_c|\psi_c\rangle\alpha_{cv} \ . \tag{5.4}$$

So, the Schrödinger equation for the pseudo wavefunction $|\varphi_v\rangle$ is written as

$$\hat{H}|\varphi_v\rangle = E_v|\varphi_v\rangle + \sum_c (E_c - E_v)|\psi_c\rangle\langle\psi_c|\varphi_v\rangle \ . \tag{5.5}$$

As a consequence, the states $|\varphi_v\rangle$ will satisfy the "Schrödinger-ish" equation with an energy-dependent pseudo-Hamiltonian

$$\hat{H}^{PK}(E) = \hat{H} - \sum_c (E_c - E)|\psi_c\rangle\langle\psi_c| \ . \tag{5.6}$$

Resulting into a pseudopotential that was proposed by Phillips and Kleinman

$$\hat{V}^{PK}(E) = \hat{V} - \sum_c (E_c - E)|\psi_c\rangle\langle\psi_c| \ . \tag{5.7}$$

Where $\hat{V}$ represents the true potential that is an effective potential in which valence electrons move.

5.2 Norm-conserving pseudopotentials

The NC pseudopotentials are a very simple procedure to extract pseudopotentials from *ab initio* atomic calculations, in which the starting point is to define a certain list of requirements, that are:

1. Real and pseudo valence eigenvalues agree for a chosen "prototype" atomic configuration.

2. Real and pseudo atomic wavefunctions agree beyond a chosen "core radius" r_c.
3. The integrals from 0 to r of the real and pseudo charge densities agree for $r > r_c$ for each valence state (norm conservation).
4. The logarithmic derivatives of the real and pseudo wavefunction and their first energy derivatives agree for $r > r_c$.

Where r_c represents the radius cutoff of the core region also, from 1, one may get

$$\varepsilon_l^{PP} = \varepsilon_{nl}^{AE} \ . \tag{5.8}$$

Also, R^{PP} is the radial part of the pseudo wavefunction and R^{AE} is the all-electron one, in which r is l-dependent (angular momentum) just like ε that is the energy-eigenvalues. Now, the combination of both 2 and 3 will lead to

$$\begin{aligned} R_l^{PP}(r) &= R_{nl}^{AE}(r) \qquad\qquad\qquad \text{, for } r > r_c \\ Q_l = \int_0^{r_c} \mathrm{dr}\ |R_l^{PP}(r)|^2 r^2 &= \int_0^{r_c} \mathrm{dr}\ |R_{nl}^{AE}(r)|^2 r^2 \quad \text{, for } r < r_c \end{aligned} \tag{5.9}$$

with Q_l being the integrated charge dependent on the radial part of the pseudo wavefunctions. Therefore one can solve the radial part of the all-electron Kohn-Sham equations in a "prototype" atomic configuration

$$\left[-\frac{1}{2}\frac{\mathrm{d}^2}{\mathrm{dr}^2} + \frac{l(l+1)}{2r^2} + v_{KS}^{AE}[n^{AE}](r)\right] r R_{nl}^{AE}(r) = \varepsilon_{nl}^{AE} r R_{nl}^{AE}(r) \ , \tag{5.10}$$

in which the KS potential is non-relativistic, also the Hartree and exchange and correlation potential are spherically approximated

$$v_{KS}^{AE}[n^{AE}](r) = -\frac{Z}{r} + v_{\mathrm{Hartree}}[n^{AE}](r) + v_{\mathrm{xc}}[n^{AE}](r) \ . \tag{5.11}$$

Finally, using the norm-conservation (5.9), the pseudo wavefunctions are determined, however, their shape in the region $r < r_c$ needs to be previously defined. Then, knowing the pseudo wavefunction, the pseudopotential will result in the inversion of the radial KS equation (5.10)

$$V_l^{scr}(r) = \varepsilon_l^{PP} - \frac{l(l+1)}{2r^2} + \frac{1}{2rR_l^{PP}(r)}\frac{\mathrm{d}^2}{\mathrm{dr}^2}[rR_l^{PP}(r)] \ . \tag{5.12}$$

Nonetheless, the resulting pseudopotential sill has screening effects caused by the valence electrons that have to be subtracted, resulting in

$$V_l(r) = V_l^{scr}(r) - v_{\text{Hartree}}[n^{PP}](r) - v_{\text{xc}}[n^{PP}](r) \ , \tag{5.13}$$

where the radius cutoff of the core region is a parameter that represents the region in which the pseudo and the true wavefunctions intercept. So the nearest that r_c is to the core, the better the pseudopotential is (hard core pseudopotential), however the efficiency of the calculus time will be lower. In other words, the radius, that defines the smoothness of the pseudopotential, must be chosen carefully to our needs.

There are several methods to construct the pseudo wavefunctions, one of them was proposed by *Troullier* and *Martins* where the pseudo wavefunctions are defined in a way that it achieves softer pseudopotentials for the d valence states of the transition metals

$$R_l^{PP}(r) = \begin{cases} R_{nl}^{AE} & \text{if } r > r_c \\ r^l e^{p(r)} & \text{if } r < r_c \end{cases} \tag{5.14}$$

with

$$p(r) = c_0 + c_2 r^2 + c_4 r^4 + c_6 r^6 + c_8 r^8 + c_{10} r^{10} + c_{12} r^{12} \ , \tag{5.15}$$

in which the coefficients are adjusted by imposing the norm-conservation, the continuity of the pseudo wavefunction and their first derivatives at $r = r_c$. Also, the screened pseudopotential has zero curvature at the origin implying that

$$c_2^2 + c_4(2l + 5) = 0 \ . \tag{5.16}$$

It is important to take into account that in some cases, when the pseudopotential is too soft, it no longer is norm-conserved.

5.2.1 Relativistic effects

Bear in mind that relativistic effects are present in a true potential, so they can be incorporated on pseudopotentials, originating shifts due to scalar relativistic effects and

spin-orbit interactions. So from the relativistic Kohn-Sham equations we can generate a pseudopotential for both $j = l + 1/2$ and $j = l - 1/2$ defining then

$$V_l = \frac{l}{2l+1}[(l+1)v_{l+1/2} + lV_{l-1/2}] \ , \tag{5.17}$$

$$\delta V_l^{so} = \frac{2}{2l+1}[v_{l+1/2} - V_{l-1/2}] \ . \tag{5.18}$$

Thus, the pseudopotential operator can be written on a semi-local form, because the PP are spherically symmetric and l-dependent, resulting in an operator that is non-local in the angular variables and local in the radial variable. In which, considering the scalar relativistic effects one obtain

$$\hat{V}_{SL} = \sum_{lm} \left|Y_{lm}\right\rangle V_l(r) \left\langle Y_{lm}\right| \ . \tag{5.19}$$

On the other hand, considering also the spin-orbit effects

$$\hat{V}_{SL} = \sum_{lm} \left|Y_{lm}\right\rangle \left[V_l(r) + \delta V_l^{so}(r)\ \mathbf{L}\cdot\mathbf{S}\right] \left\langle Y_{lm}\right| \ . \tag{5.20}$$

5.3 The Projector Augmented Wave Method

The PAW method divides space into two kind of regions, non-overlapping atomic regions, called augmentation spheres and an interstitial region, where the Kohn-Sham wavefunctions are expected to be smooth and easily described by an uniform discretization such as an uniform grid or planewaves. Despite the smooth discretization spans to the atomic regions, each atomic region has spherical augmentation functions called partial-waves. So, the total wavefunction $\varphi_k(\mathbf{r})$ is written as

$$\varphi_k(\mathbf{r}) = \tilde{\varphi}_k(\mathbf{r}) + \sum_{a}^{N_{\text{atoms}}} \sum_{nlm} c^a_{k,nlm} \left[\xi^a_{nlm}(r_a, \theta_a, \phi_a) - \tilde{\xi}^a_{nlm}(r_a, \theta_a, \phi_a)\right] \ , \tag{5.21}$$

which represents a combination of a smooth pseudo wavefunction $\tilde{\varphi}_k(\mathbf{r})$, with the atomic all-electron wavefunctions $\xi^a_{nlm}(r_a, \theta_a, \phi_a)$, subtracted by atomic pseudo wavefunctions $\tilde{\xi}^a_{nlm}(r_a, \theta_a, \phi_a)$.

Chapter 6

Methodology and Results

6.1 Methodology

In this section, the procedure to obtain our results will be discussed, focusing on three essential programs that were used in order to fulfil those objectives.

The first thing to do is to choose an element on the transition metal set from the periodic table, Chromium for example, then let us build an initial geometry. *Avogadro* is a program that has a feature that does geometry optimization based on a force field, that refers to the functional form and parameter sets used to calculate the potential energy of a system of atoms or coarse-grained particles. The geometry obtained will be a good initial educated guess. So, one picks an element using the periodic table from the program and connects 2 atoms in order to make the dimer and we optimize the geometry using the *Universal Force Field* (UFF).

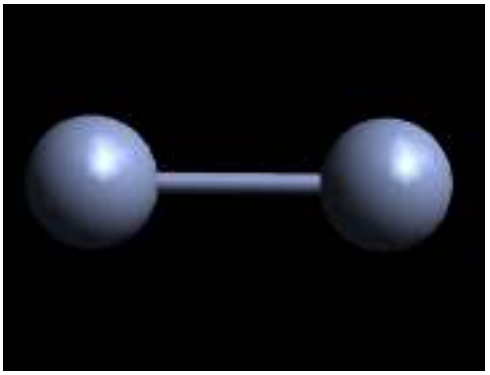

FIGURE 6.1: Example of Cr_2 dimer geometry built on *Avogadro*

Now, the first essential program is the *Atomic Pseudopotentials Engine* (APE) [36] that is a tool for generating atomic pseudopotentials within a Density-Functional Theory

framework. This program uses a logarithmic grid with two parameters a and b that are required in the two commonly used ways to construct it. The ith point of the grid is defined as $r_i = b\mathrm{e}^{ai}$ in one case and as $r_i = b\mathrm{e}^{a(i-1)}$ in the other case. The parameters a and b are determined by specifying the number of grid points and the starting and ending points. The pseudopotentials generated are Norm-conserving pseudopotentials with the method to construct the pseudo wavefunctions proposed by *Troullier* and *Martins*. Relativistic effects can be taken into account in which case the scalar-relativistic or Dirac equations are used. In order to build the pseudopotential we have to be careful on the cutoff radius that we choose since it must not be too close to the core as the computation time will not be efficient and cannot be too far away for the core, or *soft* as it will not be precise and the norm tests will fail, i.e. the norm will no longer be conserved.

The second essential program that will be used after the initial geometry and the pseudopotential is achieved is ABINIT, that allows one to find total energy, charge density and electronic structure of systems made of electrons and nuclei such as the transition metal clusters, within Density Functional theory, using pseudopotentials and using a planewave or a wavelet basis. As was said earlier, in some cases, norm-conserving pseudopotentials will be used when we can't use the PAW method, which is, when the overlap of the PAW spheres are too high to be neglected. ABINIT also includes options to optimize a geometry, according to the DFT forces and stresses. So, using a planewave basis, the eigenfunction is a periodic function that can be expanded in the complete set of Fourier components and can be written as

$$\psi_i(\mathbf{r}) = \sum_{\mathbf{k}} C_{i,\mathbf{k}} \times \frac{1}{\sqrt{\Omega}} \mathrm{e}^{\mathrm{i}\mathbf{k}\cdot\mathbf{r}} \ , \tag{6.1}$$

where $C_{i,\mathbf{k}}$ are expansion coefficients of the wavefunction in the basis of orthonormal plane waves. The independent particle Schrödinger equation in a planewave basis is

$$\hat{H}_{eff}(\mathbf{r})\psi_i(\mathbf{r}) = \left[-\frac{1}{2}\nabla^2 + V_{eff}(\mathbf{r})\right] \psi_i(\mathbf{r}) = \varepsilon_i \psi_i \ , \tag{6.2}$$

in which it is convenient to require the states to be normalized and obey periodic boundary conditions in a large volume Ω that is allowed to go to infinity. Now, in order to do the geometry optimization, it is required to do some convergence tests such as the kinetic energy cutoff, also known as ECUT that controls the number of planewaves at given k point. Basically, the larger the energy cutoff is, the better converged the calculation is. It is also required to test the cell lattice vector scalling, also known as ACELL, that gives the length scales by which dimensionless primitive translations are

to be multiplied. When using PAW, it is also necessary to do some convergence tests on the PAW energy cutoff. Finally, one obtain a geometry optimized on a given time step of molecular dynamics where the energy is minimal with all the previous parameters converged for a given magnetization. We then may repeat the procedure for another magnetization.

At last, the third program to be used is *Octopus* that is a scientific program aimed at the *ab initio* virtual experimentation. This one also describes electrons quantum-mechanically within Density Functional Theory such as the other two programs, it is also possible doing simulations in time (TDDFT). Nuclei are described classicaly as point particles. Electron-nucleus interaction is described within the pseudopotential approximation. PAW wont be used here since they are not implemented. So, despite we can use the PAW method in order to do geometry optimization, we will need a pseudopotential constructed by *APE* in order to continue the time-dependent calculation. Since *Octopus* is a program that has a real-space grid, the first step of any calculation is the determination of the grid-spacing that is necessary to converge the spectra to the required precision. A way to do the convergence test is to calculate the spectra of a cluster and change the spacing values for each spectrum as it can be shown on the following figure

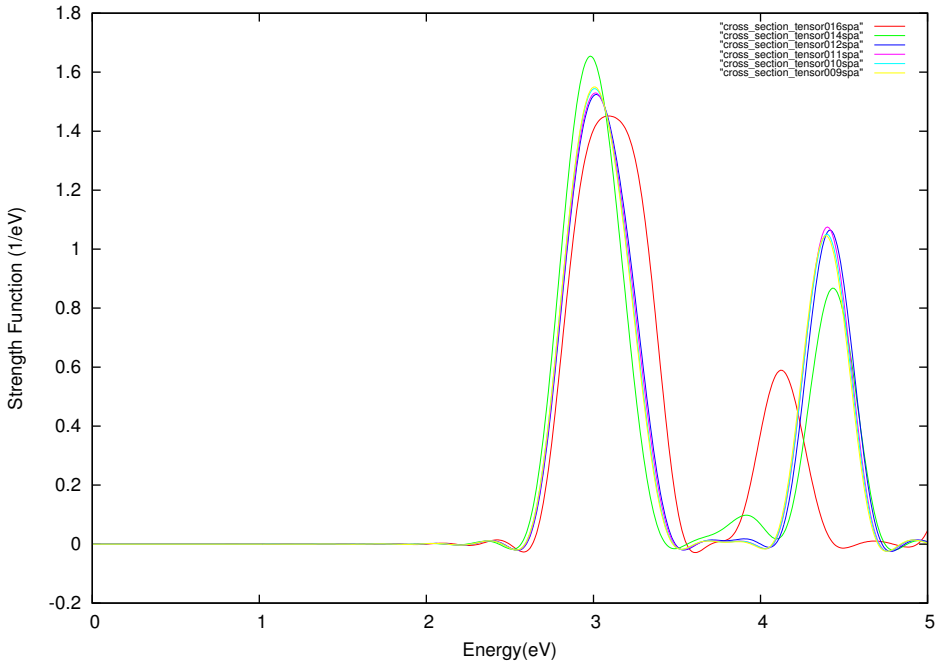

FIGURE 6.2: Chromium spectra convergence with values of spacing of 0.16, 0.14, 0.12, 0.11, 0.10 and 0.09 $\mathring{A}$.

As we can see, the spectrum is already converged on the blue line which corresponds to a spacing of 0.12 $\mathring{A}$, the less the spacing is, the more converged the spectrum is,

however, if spacing is too low, the calculation time will increase and as a consequence its efficiency will decrease. The optimum grid-spacing depends on the strength of the pseudopotential used, the deeper the pseudopotentialm the tighter the mesh has to be.

Also, we need to converge the spectra with the radius parameter, that defines the radius of the boxshape that is the shape of the simulation box, it can be a sphere, cylinder or minimum. For minimum, a different radius is used for each species, while for other shapes, the maximum is used. Since it is used the minimum boxshape, which means that the simulation box will be constructed by adding spheres created around each atom or user-defined potential. So the figure 6.3 shows the spectra convergence.

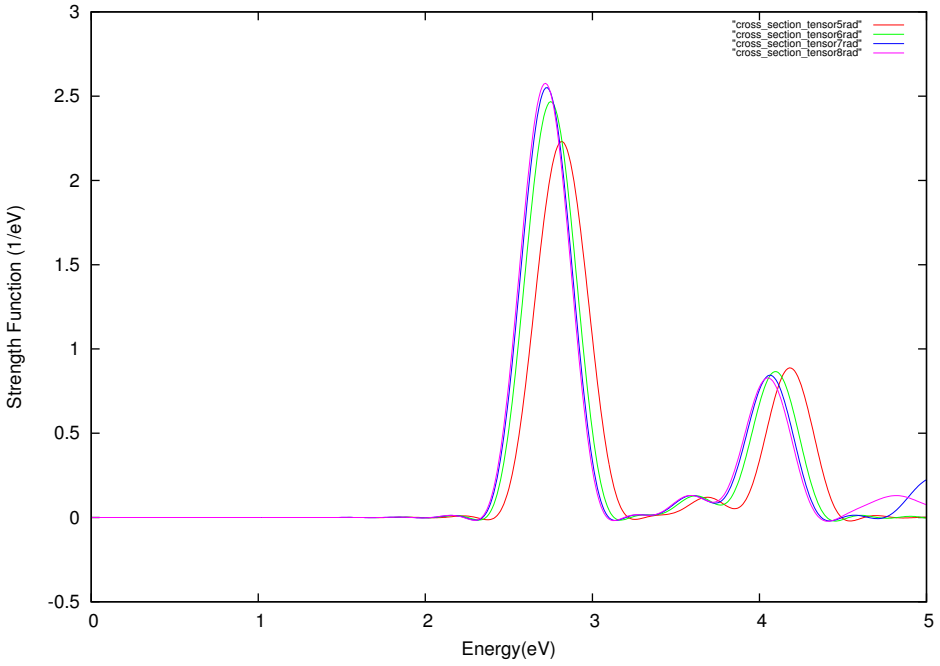

FIGURE 6.3: Chromium spectra convergence with values of radius 5, 6, 7 and 8 $\mathring{A}$.

For this case, the greater the radius is the better, however we face the same problem, if we push on the radius too much, the calculation time will not be efficient. As we can observe, the spectra is converged on the green line that is a radius value of 6$\mathring{A}$.

Finally, having the radius and spacing values for the converged spectra, we proceed to the calculation of the spectra of a given geometry with a given magnetization, we repeat after for other magnetizations that were found.

6.2 Results

In order to achieve some desired results, such as the ground-state energies, some geometries optimized and absorption spectra of some transition metal clusters, it is necessary

to proceed with the steps written on the previous section from this chapter, that is the methodology. Chromium, Manganese, Iron and Cobalt are the transition metal elements that will be focused.

6.2.1 Dimers

The most important elements that will be studied are present in the transition metal section on the periodic table, where they are known to exhibit peculiar magnetic properties, focusing in particular on Chromium, Manganese, Iron and Cobalt. It is important to mention that, due to the Chromium dimer having an incredibly low bond length, the PAW method is not precise enough since the PAW spheres will have a considerable big overlap. As a consequence, this dimer will be the only one in which the *ab initio* calculations will be done exclusively with norm-conserving pseudopotentials generated with the program *APE*.

6.2.1.1 Chromium

For the Chromium dimer (Cr_2), doing *ab initio* calculations, the geometry was optimized with the given properties.

Cluster	Magnetization $m_z(\mu_B)$	Bond Length(Å)
Cr_2	0	1.413
	Total Energy(Ha)	Atomisation Energy (Ha)
	-233.479	0.255

TABLE 6.1: Chromium properties for a null magnetization

After the ground-state calculation on *ABINIT*, the geometry obtained was used in order to get the absorption spectra within the *TDDFT* approach for the Chromium dimer with zero magnetization resulting in

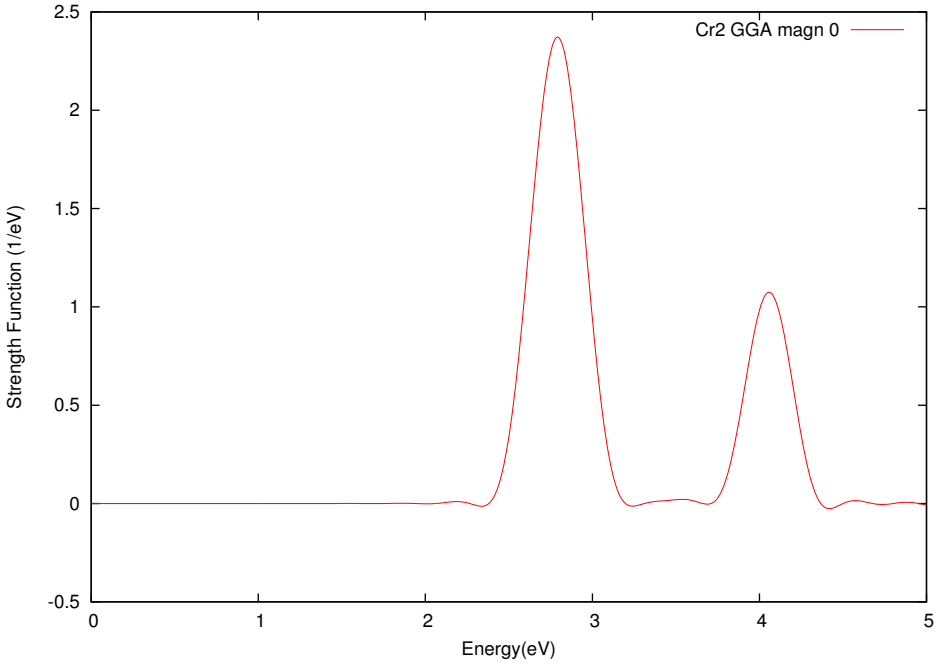

FIGURE 6.4: Absorption Spectrum for Cr_2 with $m_z = 0$

As we can see, there are two major peaks about 2.85 and 4.1 eV, also, it seems to have minor peaks near the major ones, however, even after a calculation with increased resolution, those peaks are hardly noticeable so these ones have low statistical weight on the spectrum, which means that the transition probability from the ground-state to those excited states is low. This spectrum, such as all the other ones obtained, was achieved by using *NCPP* with the *explicit PBE* form of the *GGA* exchange and correlation functionals. Also, the intensity of the first peak is greater than the second, witch means that an electron is more likely to make a transition.

Doing the calculations with the *LDA xc* functionals, we obtain spectra that can be compared as the figure 6.5 shows.

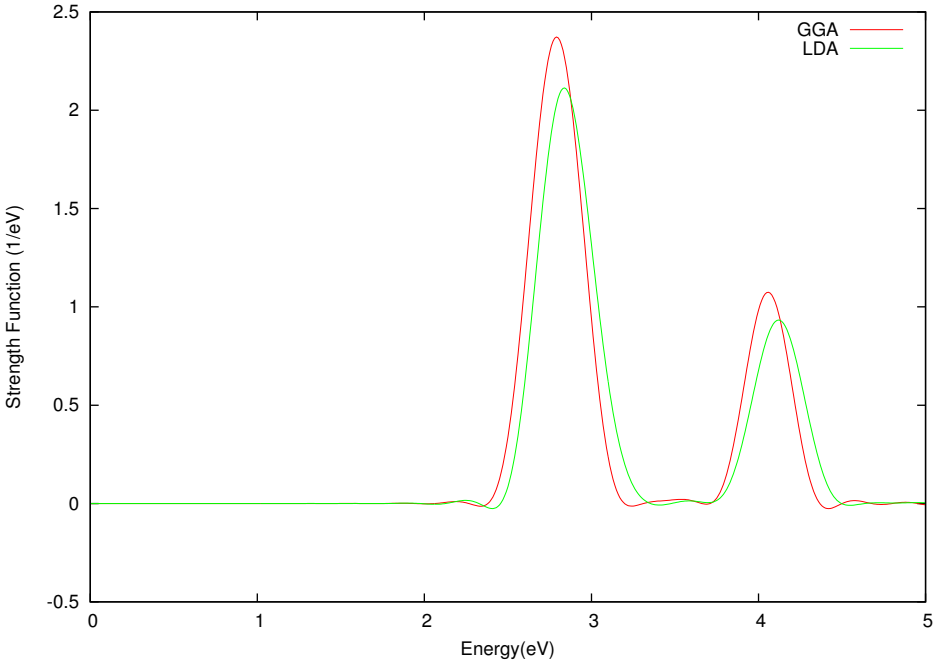

FIGURE 6.5: Absorption Spectra for Cr_2 with $m_z = 0$, using different exchange and correlation functionals, LDA on the green line and GGA on the red one

If we compare then the figure 6.5, one may notice that the major peaks are located at about the same energies with about the same intensity ratio between both of them so, as was mentioned on section 3.4, GGA and LDA will produce similar approximations on exchange and correlation functionals.

Now, if the cluster has a different magnetization, i.e. other than zero, we can observe different properties (Tab. 6.2).

Cluster	Magnetization $m_z(\mu_B)$	Bond Length(Å)
Cr_2	2	1.428
	Total Energy(Ha)	Atomisation Energy (Ha)
	-233.496	0.272

TABLE 6.2: Chromium properties for a given magnetization

Where the total energy lowers from -233.479 to -233.496 Ha, being then $\Delta E = 0.017$ Ha with the increase of m_z from 0 to 2, there is also a slightly increase on the bond length as we can observe in figure 6.6.

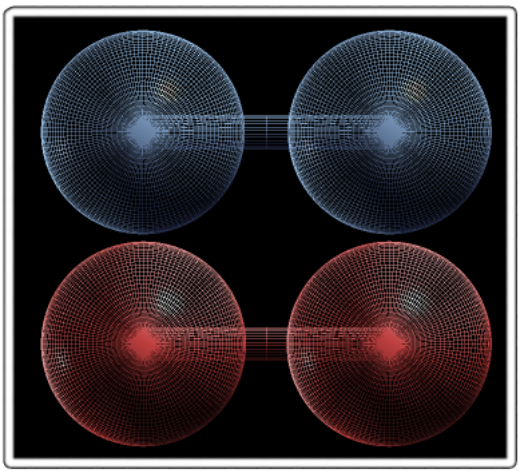

FIGURE 6.6: Chromium dimer bond length comparison with different magnetizations where the blue dimer represents the Cr_2 with $m_z = 2$ and the red one represents Cr_2 with $m_z = 0$

Since the difference in the bond length is very low, we cannot notice any.

Now, using *Octopus* with the geometry obtained with a magnetization other than zero, $m_z = 2\ \mu_B$ in this case, one can get a different spectrum as the figure 6.7 shows.

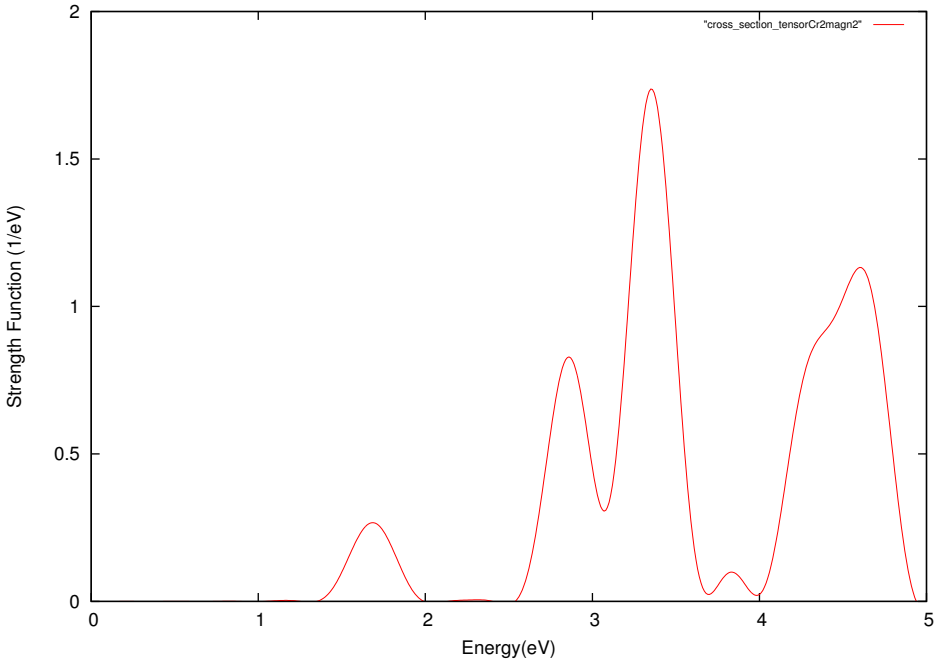

FIGURE 6.7: Absorption Spectrum for Cr_2 with $m_z = 2$

As we can observe, four peaks are explicitly represented between 1 and 4 eV where the first one is located around 1.7 eV, the second around 2.85 eV and the third and fourth around 3.4 and 3.8 eV respectively, we may also notice a peak with a non-usual

form around 4.6 eV this one may represent two peaks merged together, increasing the resolution of the calculation by adding more time steps may correct the problem, however the computation time would greatly increase and the resolution is already pushed to the limit. We can compare now the spectra of the same dimer with different magnetizations with the respective bond lengths, analysing figure 6.8.

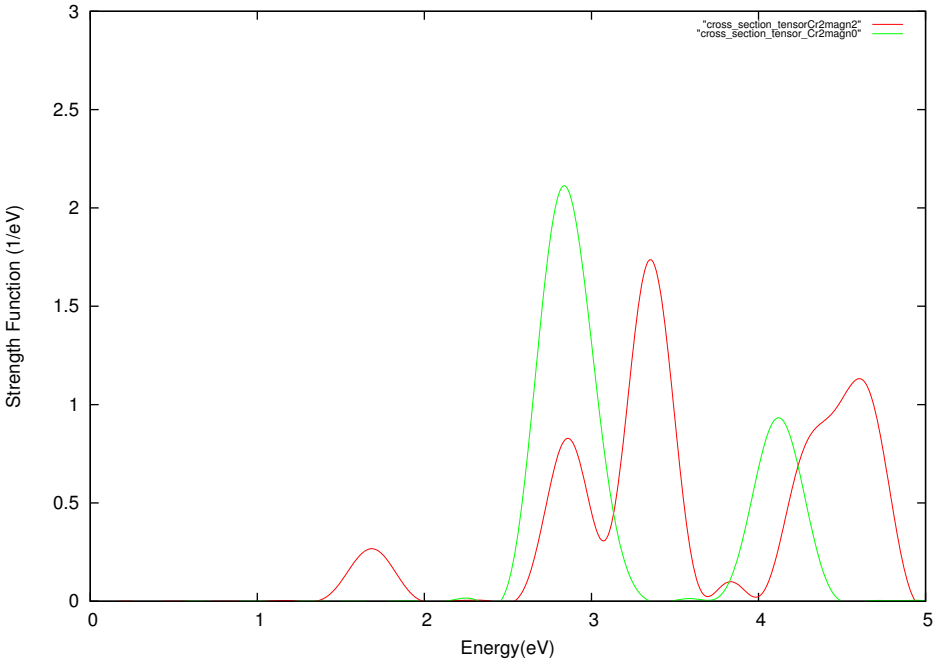

FIGURE 6.8: Comparison between absorption spectra for Cr_2 with $m_z = 0$ and $m_z = 2$

The green line represent the dimer with $m_z = 0\ \mu_B$ and the red one represents $m_z = 2\ \mu_B$. As we can observe, if the dimer has a magnetization, more peaks are produced, however, one of them coincides with a peak from the null magnetization spectrum, around 2.85 eV, despite the difference in the intensity. So, one may conclude that the difference in the magnetization of one dimer will not only influence its bond length but also will influence its absorption spectra by having a larger set of energies where it is likely to have a transition to a excited state.

6.2.1.2 Manganese

Repeating the *ab initio* calculations for the manganese dimer with zero magnetization, one may find the properties shown on table 6.3

Cluster	Magnetization $m_z(\mu_B)$	Bond Length(Å)
Mn_2	0	2.737
	Total Energy(Ha)	Atomisation Energy (Ha)
	-209.373	0.837

TABLE 6.3: Manganese properties for a null magnetization

Since the bond length of the manganese dimer is much greater than the chromium, we wont get any problem with the overlap of the PAW spheres, so in order to save time, the geometry was optimized using the PAW method. The procedure to obtain the absorption spectra is the same as for the Chromium, we use the *TDDFT* approach with the geometry obtained from *ABINIT*, producing figure 6.9.

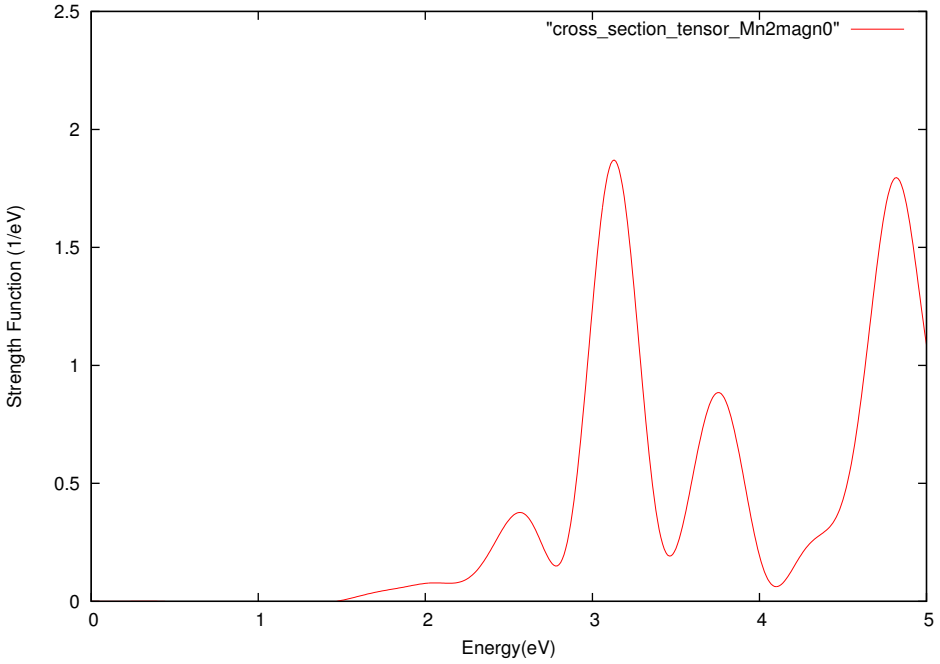

FIGURE 6.9: Absorption Spectrum for Mn_2 with $m_z = 0$

This spectrum has slightly more peaks than the one produced with the Chromium dimer with null magnetization, there is four well defined peaks between the energy of 1 and 5 eV, being the first one around 2.55 eV, the second and the third ones aroud 3.1 and 3.75 eV, finally the fourth one on 4.8 eV, where the second and the last one have higher intensities than the rest of the peaks, which means that there is more likely to have a transition around these energies.

Another geometry was found for the Manganese dimer, with $m_z = 2\ \mu_B$, that have properties specified on the table 6.4.

Cluster	Magnetization $m_z(\mu_B)$	Bond Length(Å)
Mn_2	2	2.345
	Total Energy(Ha)	Atomisation Energy (Ha)
	-209.363	0.847

TABLE 6.4: Manganese properties for a given magnetization

Comparing both the properties of the Chromium dimer with the two different magnetizations, with the ones of the Manganese dimer, one may notice that the total energy of the Manganese dimer, on the contrary that was shown to the Chromium dimer, increases with the increase of the magnetization, being $\Delta E = 0.374$ Ha. Also, instead of the bond length is increased such as the Chromium dimer, it decreases, as the figure 6.10 shows.

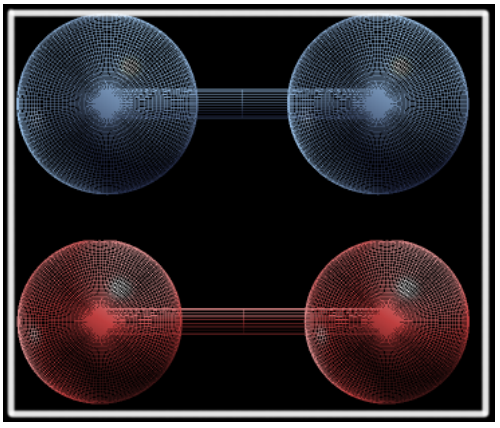

FIGURE 6.10: Manganese dimer bond length comparison with different magnetizations where the blue dimer represents the Mn_2 with $m_z = 2$ and the red one represents Mn_2 with $m_z = 0$

One can also notice that in this case, the differences between the bond lengths are quite noticeable.

6.2.1.3 Iron

The properties of the Iron cluster are obtained when the geometry is optimized using *ABINIT* and are show in the table 6.5.

Cluster	Magnetization $m_z(\mu_B)$	Bond Length(Å)
Fe_2	0	2.246
	Total Energy(Ha)	Atomisation Energy (Ha)
	-248.562	0.598

TABLE 6.5: Iron properties for a null magnetization

The bond length of the Iron dimer is similiar to the manganese one when comparing with the Chromium cluster, so, for the same reasons that the PAW method was used for the Manganese, it will be also used for the Iron cluster. The absorption spectrum is then represented by the figure 6.11.

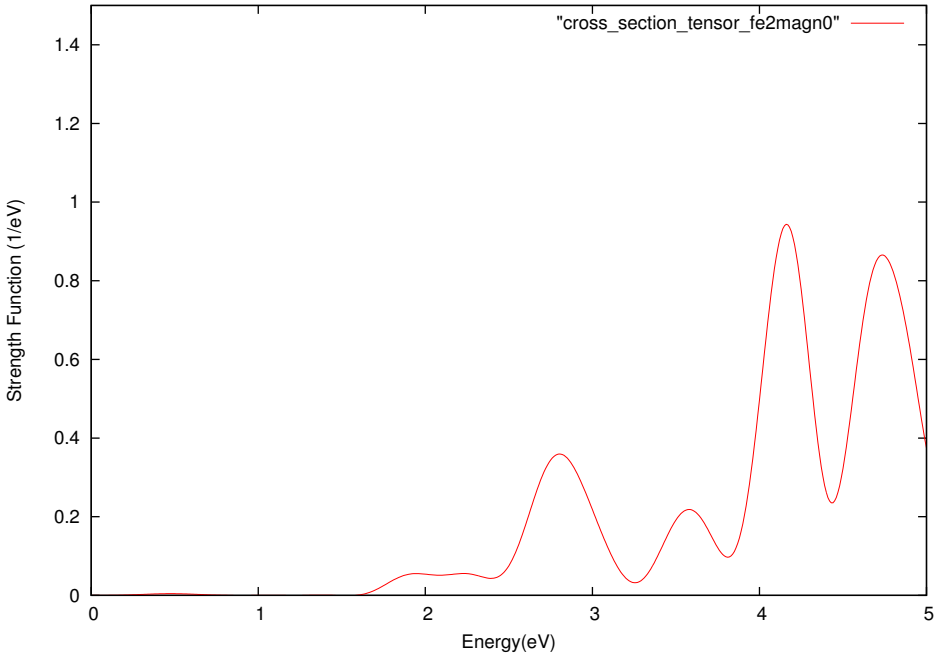

FIGURE 6.11: Absorption Spectrum for Fe_2 with $m_z = 0$

The spectrum for the Iron dimer, also has four salient peaks between the energies of 2 and 5 eV, where the first two located around 2.8 and 3.6 eV, and the last two ones have a higher intensity, located around 4.15 and 4.8 eV, however, their intensities are weaker when compared with the absorption spectra of the other clusters.

Using once again the *ABINIT* it was found a geometry for the same cluster with a magnetization that differs from zero with the properties stated in the table 6.6.

Cluster	Magnetization $m_z(\mu_B)$	Bond Length(Å)
Fe_2	2	2.036
	Total Energy(Ha)	Atomisation Energy (Ha)
	-248.562	0.598

TABLE 6.6: Iron properties for a given magnetization

The difference between the total energies of the Iron dimer with null magnetization and the Iron dimer with $m_z = 2\ \mu_B$ are in the order of 1×10^{-4} Ha, so with the change of the magnetization, the total energy remain approximately the same, however the bond length decreases about 0.2 $\mathring{A}$ as it is represented in the figure 6.12.

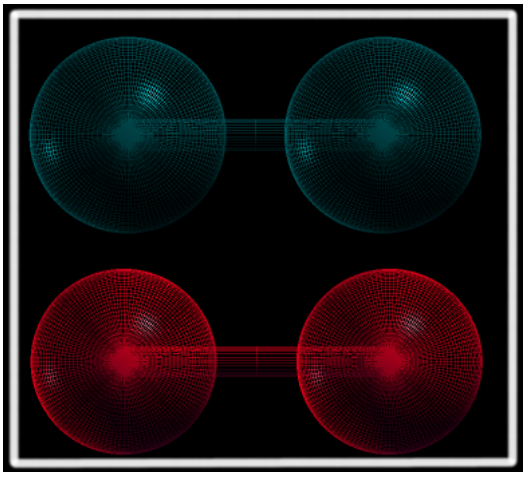

FIGURE 6.12: Iron dimer bond length comparison with different magnetizations where the blue dimer represents the Fe_2 with $m_z = 2$ and the red one represents Fe_2 with $m_z = 0$

The absorption spectrum obtained for the Iron dimer with $m_z = 2$ is shown in figure 6.13.

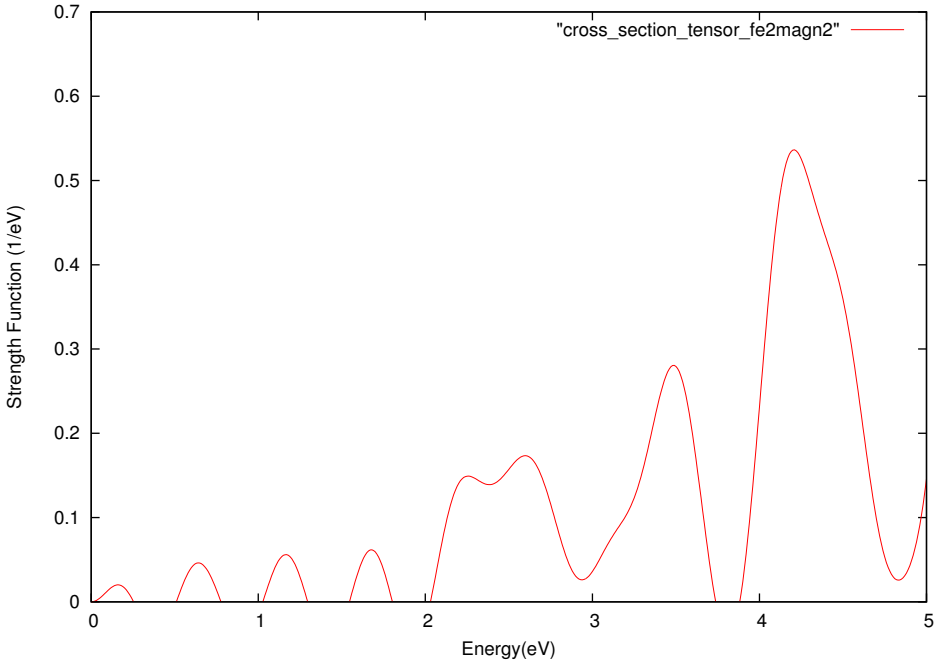

FIGURE 6.13: Absorption Spectrum for Fe_2 with $m_z = 2$

One can notice that this spectrum has several peaks with low statistical weight within the interval $[0 : 3]$ eV, also there are other two peaks with a significant intensity around 3.5 eV and 4.2 eV.
In order to compare both absorption spectra obtained for Iron dimer, the figure 6.14 is produced.

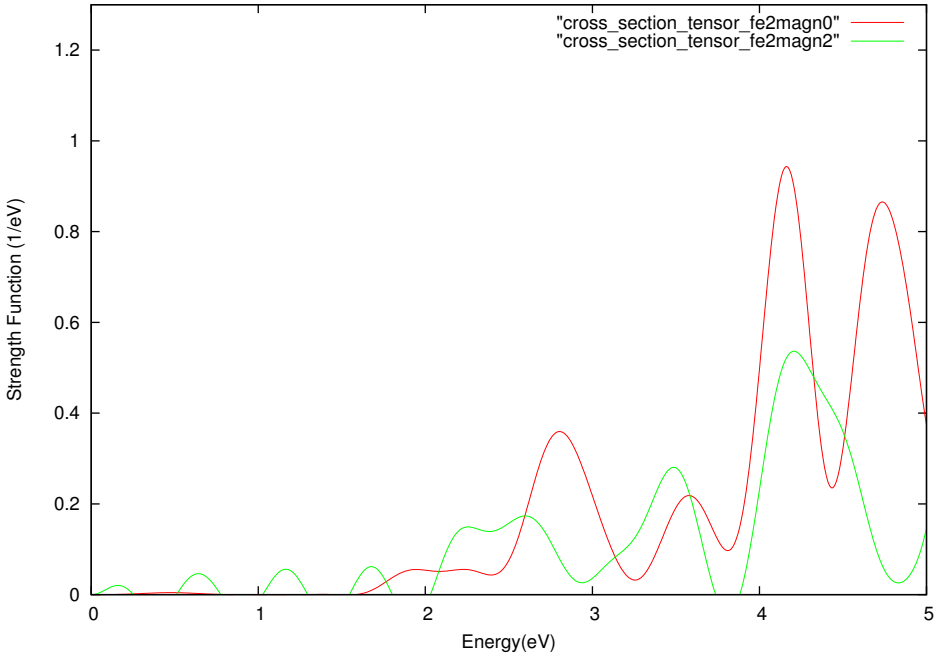

FIGURE 6.14: Comparison between absorption Spectra for Fe_2 with $m_z = 0$ and $m_z = 2$

The red line represents the absorption spectrum for the Iron dimer with null magnetization and the green line represents the absorptions spectrum for the same dimer with $m_z = 2$. Comparing both spectra, one can notice that there are two peaks that coincide on approximately the same energies, around 3.5 and 4.2 eV but with different intensities. The dimer with null magnetization has more relevant peaks that the one with $m_z = 2$, having other one around 2.8 eV.

6.2.1.4 Cobalt

For the Cobalt dimer, a geometry for a null magnetization was obtained, in which its properties are represented in the table 6.7.

Cluster	Magnetization $m_z(\mu_B)$	Bond Length(Å)
Co_2	0	2.157
	Total Energy(Ha)	Atomisation Energy (Ha)
	-292.505	0.151

TABLE 6.7: Cobalt properties for a null magnetization

The Cobalt, Manganese and Iron clusters have similar bond lengths when comparing with the Chromium so, It was also used the PAW method instead of the norm-conserving pseudopotential in order to do the *ab initio* calculations. The absorption spectrum of the dimer is represented in figure 6.15.

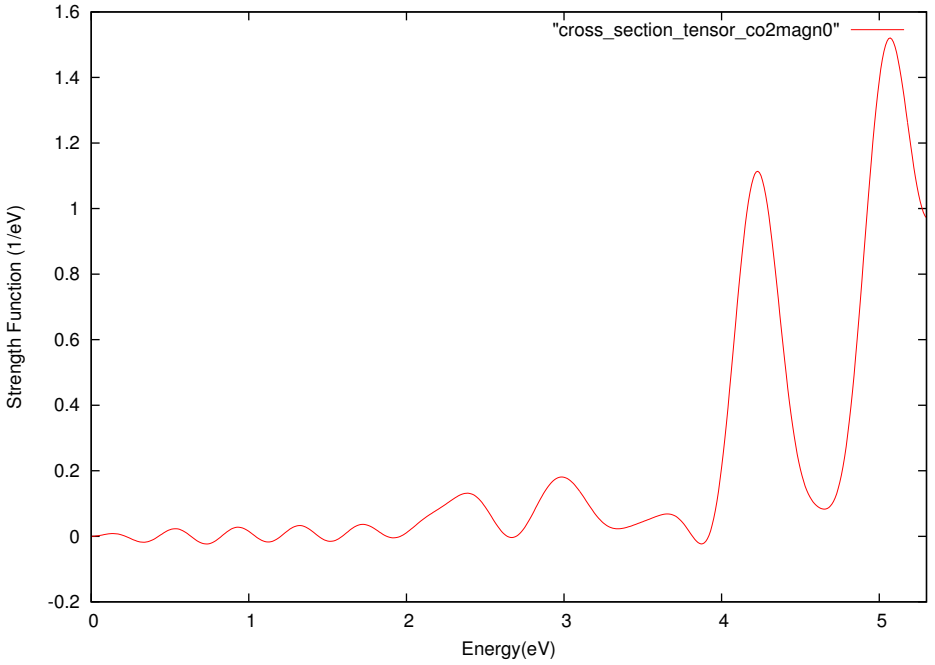

FIGURE 6.15: Absorption Spectrum for Co_2 with $m_z = 0$

As we can observe, this spectrum is the one with the highest number of peaks yet, most of them have such small intensities that can be neglected, having then two major peaks, one around 4.2 eV and the other one around 5.1 eV.

Unfortunately, a geometry with a magnetization other than zero for the Cobalt dimer was not found.

Chapter 7

Conclusion

In this work, the *Time-dependent Density Functional Theory* approach was used in order to do calculations regarding not only the ground-state of transition metal clusters, but also its excited states, that are important in order to identify its optical and magnetic properties. Analyzing the *optical absorption spectra*, one may conclude that the Chromium dimer is the cluster with the lowest number of peaks, it however has one that has the highest intensity, also, when we change the magnetization, a characteristic peak appears in the red zone. Manganese has two peaks with relevant intensities, the other clusters have shown to have some more peaks but with less relevant intensities to be taken into account. Also, this work have shown that magnetizations other than null will change the quality of the spectrum, since it may produce more peaks and change the intensity of some relevant peaks, which means that the transition probability to an excited state is changed.

Analyzing the Iron dimer, it is important to take into account that Iron clusters are known to exhibit ferromagnetic configurations, this work concludes that it can also exhibit antiferromagnetic configurations since a geometry with a null magnetization was found for the dimer.

At last, in my opinion, Manganese is the cluster with the best absorption spectra since it has the best ratio of number of peaks and its intensities, also it is expected that the spectrum changes with the change in the magnetization as was observed in the other ones. So one may conclude that from all the dimers studied in this work, the best materials to construct spintronic devices are Manganese and Chromium.

Due to the high computational time required in order to run the programs, some convergence problems and such, unfortunately there was not enough time to study all the

magnetizations and clusters with higher number of atoms, like trimers and pentamers that were initially proposed.

Bibliography

[1] Claude Cohen-Tanoudji, Bernard Diu and Franck Laloë. *Quantum Mechanics* . Volume One, 1977.

[2] Claude Cohen-Tanoudji, Bernard Diu and Franck Laloë. *Quantum Mechanics*. Volume Two, 2005.

[3] Richard M. Martin. *Electronic Structure Basic Theory and Practical Methods*. Cambridge University Press, 2004.

[4] Neil W. Ashcroft and N. David Mermin. *Solid State Physics*. Cornell University, 1976.

[5] C. Fiolhais, F. Nogueira and M. Marques. *A Primer in Density Functional Theory*. Lecture Notes in Physics, Springer, 2003.

[6] M.A.L. Marques, C.A. Ullrich, F. Nogueira, A. Rubio, K. Burke, E.K.U. Gross. *Time-Dependent Density Functional Theory*. Lecture Notes in Physics, Springer, 2006.

[7] M.A.L. Marques, C.A. Ullrich, F. Nogueira, A. Rubio, K. Burke, E.K.U. Gross. *Time-Dependent Density Functional Theory*. Lecture Notes in Physics, Springer, 2006.

[8] Micael J.T. Oliveira, Fernando Nogueira. *Generating relativistic pseudo-potentials with explicit incorporation of semi-core states using APE, the Atomic Pseudo-potentials Engine*. Center of Computational Physics, University of Coimbra, 2007.

[9] Patrizia Calaminci. *Density functional theory optimized basis sets fro gradient corrected functionals: 3d transition metal systems*. The journal of chemical physics, 2007.

[10] Christoph R. Jacob and Markus Reiher. *Spin in Density-Functional Theory*. Karlsruhe Institute of Technology (KIT), 2012.

[11] Micael J. T. Oliveira, Paulo V. C. Medeiros, José R. F. Sousa, Fernando Nogueira and Gueorgui K. Gueorguiev. *Optical and magnetic excitations of metal-encapsulating Si cages: A systematic study vy time-dependent density dunctional theory.* Center for Computational Physics, University of Coimbra, 2013.

[12] Alberto Castro, Miguel A. L. Marques, Julio A. Alonso, George F. Bertsch, K. Yabana and Angel Rubio. *Can optical spectroscopy directly elucidate the ground state of C_{20}?.* Journal of Chemical Physics volume 116 number 5, 2002.

[13] Robert van Leeuwen. *Density functional approach to the many-body problem: key concepts and exact functionals.* Theoretical Chemistry, Materials Science Centre, Nijenborgh, 2003.

[14] Nicola Spallanzani. *Time Dependent DFT Investigation of Optical Properties and Charge Dynamics In Light-Harvesting Assemblies.* Università degli Studi di MODENA e GEGGIO EMILIA.

[15] Miguel A. L. Marques and E. K. U. Gross. *Time-Dependent Density Functional Theory.* The Journal of Chemical Physics, 2008.

[16] G. Rollmann and P. Entel. *Electron correlation effects in small iron clusters.* Computing Letters vol. 1, no. 4, 2004.

[17] Sanjubaka Sahoo. *Ab initio study of free and deposited transition metal clusters.* Universität Duisburg-Essen, 2011.

[18] Peter Elliott, Kieron Burke and Filipp Furche. *Excited states from time-dependent desity functional theory.* University of California and Karlsruhe, 2007.

[19] Tiago Cerqueira. *Influence of the Exchange and Correlation Functional in the Ionization Potentials of Atoms.* Department of Physics, faculty of sciences and technology, University of Coimbra, 2012.

[20] Mário Rui Gonçalves Marques. *Optical and Magnetical Properties of Endohedral SIlicon Cages.* Department of physics, University of Coimbra, 2015.

[21] D. R. Hamann, M. Schlüter and C. Chiang *Norm-Conserving Pseudopotentials.* Physical Review Letters Volume 43, Number 20, 1979.

[22] Micael José Tourdot de Oliveira. *Relativistic effects in the optical response of low-dimensional structures: new developments and applications within a time-dependent density functional theory framework.* Faculdade de Ciências e Tecnologia da Universidade de Coimbra, 2008.

[23] Alberto Castro, Miguel A. L. Marques, Julio A. Alonso, Angel Rubio. *Optical properties of nanostructures from time-dependent density functional theory*. Journal of Computational and Theoretical Nanoscience, vol 1, 1-24, 2005.

[24] C. Kohl and G. F. Bertsch. *Noncollinear magnetic ordering in small chromium clusters*. Physical Review B, 1999.

[25] Pedro Miguel Monteiro Campos de Melo. *Orbital dependent functionals in non-collinear spin systems*. Department of Physics, University of Coimbra, 2012.

[26] Robertson Wesley Burgess. *A TDDFT Study of the Optical Absorption Spectra of Gold and Silver Clusters*. University of Newcastle, 2012.

[27] Florian Gregor Eich. *Non-collinear magnetism in Density-Functional Theories*. Im Fachbereich Physik der Freien Universität Berlin eigereichte, 2012.

[28] Florian Gregor Eich. *Atomic ionization energies with hybrid functionals*. Department of Physics, University of Coimbra, 2014.

[29] Veerle Vanhoof. *Density Functional Theory Studies for Transition Metals: Small (Fe,Co)-clusters in fcc Ag, and the Spin Density Wave in bcc Chromium*. Instituut voor Kern en Stralingsfysica, 2006.

[30] Carsten A. Ullrich. *Time-Dependent Density-Functional Theory Concepts and Applications*. Oxford University Press, 2005.

[31] M.A.L Marques, C.A. Ullrich, F. Nogueira, A. Rubio, K. Burke, E.K.U. Gross. *Time-Dependent Density Functional Theory* . Lecture Notes in Physics, Vol. 706, 2006.

[32] Eberhard Engel, Reiner M. Dreizler. *Theoretical and Mathematical Physics Density Functional Theory An Advanced Course* . Springer, Series 720, 2005.

[33] Robert G. Parr and Weitao Yang. *Density-Functional Theory of Atoms and Molecules*. Oxford University Press, 1989.

[34] Attila Szabo and Neil S. Ostlund. *Modern Quantum Chemistry Introduction to Advanced Electronic Structure Theory*. Donver Publications, 1989.

[35] Kieron Burke and friends. *The ABC of DFT*. Department of Chemistry, University of California, 2007.

[36] Micael Oliveira and Fernando Nogueira. *The APE manual*. Coimbra, 2008.